Review

Developments of Core/Shell Chitosan-Based Nanofibers by Electrospinning Techniques: A Review

Siriporn Taokaew [1,]*[ ] and **Tapanee Chuenkaek** [2]

[1] Department of Materials Science and Bioengineering, School of Engineering,
Nagaoka University of Technology, Nagaoka 940-2188, Niigata, Japan
[2] Department of Science of Technology Innovation, Nagaoka University of Technology,
Nagaoka 940-2188, Niigata, Japan; s185002@stn.nagaokaut.ac.jp or c.tapanee@gmail.com
[*] Correspondence: t.siriporn@mst.nagaokaut.ac.jp or siriporntaokaew@gmail.com

Abstract: This review is focused on the recent development of various chitosan-based nanofibers (membranes, patches, mats, and scaffolds) that have been designed into core and shell structures using emulsion and coaxial electrospinning techniques. Chitosan, a promising polysaccharide derived from natural sources, holds potential for diverse applications, including nanofiber production, aimed at fostering sustainability. Core/shell chitosan-based nanofibers offer appealing features, including drug encapsulation and sustained release capabilities, with a higher efficiency than uniaxial fibers. The fabrication of core/shell chitosan-based nanofibers, including the co-spinning agents and various spinning parameters, such as spinning voltage, needle size, spinning flow rate, distance from needle tip to collector, temperature, and humidity, is summarized in this work. The review also explores updated applications in various fields, such as textiles, medical dressings, drug release systems, filtration membranes, and food packaging. It highlights the current advancements in core/shell chitosan-based nanofibers produced via electrospinning techniques. The innovative insights presented in the recent literature and the challenges associated with these sustainable materials are thoroughly examined, offering valuable contributions to the field.

Keywords: chitosan; coaxial electrospinning; emulsion electrospinning; nanofiber; core/shell structure

1. Introduction

The use of biopolymer material alternatives to replace conventional plastics and non-renewable materials is a key component of the United Nations' Sustainable Development Goals (SDGs) [1]. Bio-based products can be used to replace conventional fossil fuel-based products, such as plastics, in order to transition from a wasteful linear economy to a sustainable circular economy [2]. Approximately 98% of single-use plastic products originate from fossil fuels, with around 85% eventually ending up in landfills or as unregulated waste [2]. In 2019 alone, 6.1 million tons of plastic waste infiltrated aquatic environments, 1.7 million tons flowed into oceans, and an additional 109 million tons accumulated in rivers [3]. The accumulation of plastics in rivers suggests a continued flow into oceans for decades to come, even with substantial reductions in mismanaged plastic waste. Furthermore, the forecasted growth in greenhouse gas emissions associated with the production, use, and disposal of conventional petroleum-based plastics is expected to reach 19% of the global carbon budget by 2040 [2]. However, sustainable alternatives can mitigate the buildup of single-use plastics in the environment due to biodegradability [1]. Among different biopolymers, chitosan has been widely considered a good candidate for numerous everyday applications, e.g., plastic replacement [4,5]. Chitosan is a linear cationic polymer comprising randomly distributed N-acetyl glucosamine and glucosamine units, derived from the deacetylation of chitin. Chitin is abundantly found in the exoskeletons of crustaceans, such as crab and shrimp shells [6,7]. The renewability, biodegradability, biocompatibility, low-cost, and

antimicrobial properties of chitosan are influential in its selection as a raw material [8,9]. The applications of chitosan include textiles [10–12], medical dressings/scaffolds [13–20], water/air purification materials [21–27], and food storage products [28–32]. Moreover, chitosan has a higher solubility than chitin, which is not soluble in water or chemical solvents because of the higher proportion of N-acetylglucosamine units. The increased proportion of glucosamine units in chitosan facilitates its solubility in dilute aqueous acidic solutions below its pKa (pH = 6.5), which includes acids like acetic, formic, and lactic acids [33]. Due to its solubility, chitosan has versatility in different forms, such as powder, membranes, sheets, films, and fibers [34].

Utilizing green chemistry for nanomembrane fabrication presents a promising approach to reducing the reliance on petroleum-based membranes. In the last few decades, the development of renewable fibrous biopolymeric membranes has expanded significantly for a wide range of applications [35]. There are various methods to produce fiber materials, such as gel-state fiber forming, solution blowing, melt-spinning [36], microfluidics [37], and solution spinning [38]. Spinning techniques include dry-jet wet spinning, dry spinning, wet spinning, gel spinning, melt-spinning, and electrospinning [39]. The forces used can be classified into pressurized air, centrifugal forces, and electric voltage to eject a jet of polymer solution or melt from the nozzle tip and to deposit the produced fibers on the collector [40–42]. Among the spinning techniques used to produce biopolymer fibers, electrospinning is widely used as a low-cost method for producing submicron and nanometric fibers [43]. The cumulative number of publications involving the electrospinning of chitosan has grown each year in the last decade, as shown in Figure 1A. The data also show that the electrospinning of chitosan has a wide range of applications in various fields (Figure 1B). The electrospinning process is influenced by three primary factors: polymeric solution characteristics, processing conditions, and environmental parameters. In electrospinning, the application of a high-electric field amplifies the repulsive forces between ionic groups within the polymer structure, resulting in the formation of noncontinuous fibers and beads. Additionally, the formation of a three-dimensional network, supported by hydrogen bonding, impedes the movement of polymeric chains when subjected to an electrical field [33]. Therefore, electrospinning of polyelectrolytes, such as chitosan, in acidic solvents is difficult. To enhance spinnability, chitosan nanofibers have been developed by blending chitosan with synthetic polymers, such as polyethylene oxide (PEO), poly(ε-caprolactone) (PCL), polyvinyl alcohol (PVA), polylactic acid (PLA), poly-L-lactic (PLLA), poly(lactic-co-glycolic) acid (PLGA), and polyvinylpyrrolidone (PVP) [18,44–47]. Moreover, the incorporation of both chitosan and synthetic polymers can yield hybrid fibers with advantageous properties derived from the strengths of each polymer. This includes the biological activities inherent in chitosan and the mechanical properties characteristic of synthetic polymers. There are three main electrospinning techniques, namely, uniaxial electrospinning, emulsion electrospinning, and coaxial electrospinning, based on how active components are embedded to prepare hybrid chitosan nanofibers. Emulsion and coaxial electrospinning are two methods used for fabricating hybrid nanofibers with a core/sheath structure. In this configuration, the outer shell layer can encapsulate and effectively control the release of active components contained within the inner core [48,49]. Besides higher encapsulation efficiency than uniaxial electrospinning, the enhanced stability and functionality of encapsulated active components are the main advantages of these electrospinning procedures [50,51]. With the superior characteristics of chitosan and the unique characteristics of the core/shell, recent attention has been directed toward this structure of chitosan-based nanofibers for improved functional performance. Particularly, the core/shell chitosan fibers have been utilized in various specific applications, including enhancing the biocompatibility of scaffolds in tissue engineering with a more biocompatible chitosan shell [52], controlling drug release by tailoring the core and shell matrices [53], and protecting sensitive biomolecules used for food packaging [54].
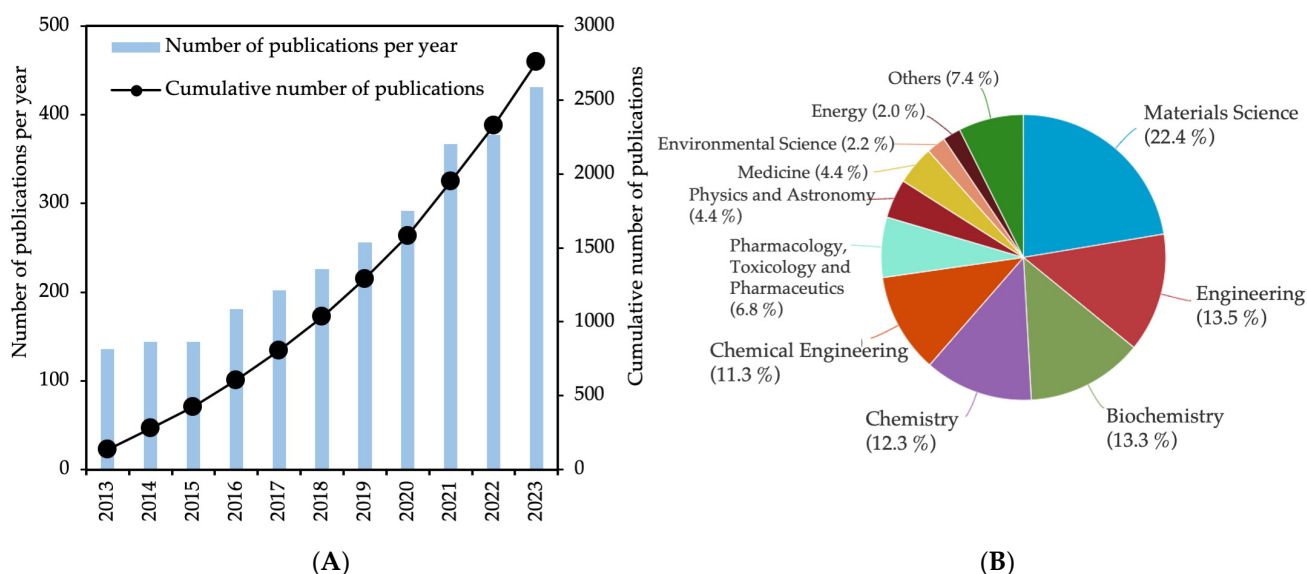
Figure 1. Number of publications by year from 2013 to 2023 (**A**) and percent of publications by subject area (**B**) in the Scopus platform using the keywords "chitosan" and "electrospinning".

Recently, numerous efforts have been undertaken to technically advance the development of innovative and sustainable core/shell chitosan-based nanofibers using electrospinning techniques. A series of co-spinning agents and spinning parameters have been proposed, and their high applicability in biomedical, pharmaceutical, environmental, and food packaging applications has been proven. This review provides a comprehensive overview of the latest advancements in core/shell chitosan-based nanofibers fabricated via electrospinning techniques. It aims to offer innovative insights by synthesizing new findings from recent research, focusing particularly on studies conducted in the past five years.

2. Overview of Electrospinning of Chitosan

Electrospinning is a spinning method that uses the power of an electric field to produce continuous, fine fibers from a polymeric solution while also controlling the deposition of these polymer fibers onto target substrates [55]. It has become a fast-growing technique for fabricating nanocomposites at the nanoscale [56]. Fabrication of nanofibers, with average diameters spanning from tens to hundreds of nanometers, is affected by electrospinning parameters [57]. Those parameters are electric field, spinning distance from the needle to the collector, needle diameter, flow rate, collector type, solution (solvent type, solvent volatility, concentration of polymer, molecular weight/branching of polymer, solution conductivity, viscosity, and surface tension), and the surrounding environment (such as temperature, air flowrate, and relativity humidity (RH)) [58–61].

Electrospinning devices typically consist of a syringe pump, an electrically conductive spinneret, a grounded collector, and a high-voltage power supply (Figure 2). These key components can be configured in either a horizontal or vertical orientation [55]. Before spinning, the polymer, such as chitosan, is dissolved in a volatile solvent and added to the syringe. The solution(s) flow through needle(s) connected to a voltage source, which is simultaneously linked to a collector. The flow rate and volume of the polymer solution are manipulated by the syringe pump and the flow rate controller [62]. Chitosan nanofibers are formed as the solvents evaporate while the liquid jet travels through the air and are collected as electrospun nanofibrous membranes on an electrically grounded target [63]. The collector plays a crucial role in electrospinning. Choosing an appropriate collector is essential, with options including drum, plate, parallel plate, cocoon, disc, and conic collectors, and primarily depends on the applications of the nanofibers. For the fabrication of chitosan nanofibers, two collector geometries, namely, a rotating metallic drum and a metallic plate collector, are commonly employed to obtain nanosized fibers [14,16].

Chitosan nanofibers produced using the flat plate collector exhibit a distribution with random orientation. The rotating drum setup facilitates controlled and organized fiber deposition, allowing the production of desired nanofiber characteristics, including both random and aligned configurations, by adjusting the rotation speed [52]. A common setup is a syringe containing a homogeneous spinning solution and a needle serving as the spinneret, also known as "uniaxial electrospinning" or "blend electrospinning", to form monoaxial nanofibers [59]. When emulsion is used as the polymer solution loaded in a syringe or "emulsion electrospinning", core/shell nanofibers are formed [64,65] (Figure 2A). Two syringes/nozzles for "coaxial electrospinning" are also used to fabricate the core/shell structure by loading core and shell materials into the different syringes [53,66] (Figure 2B). A method of "side-by-side electrospinning" (Figure 2C) to create a dual-compartment system to prepare Janus chitosan nanofibers has not been found [67].
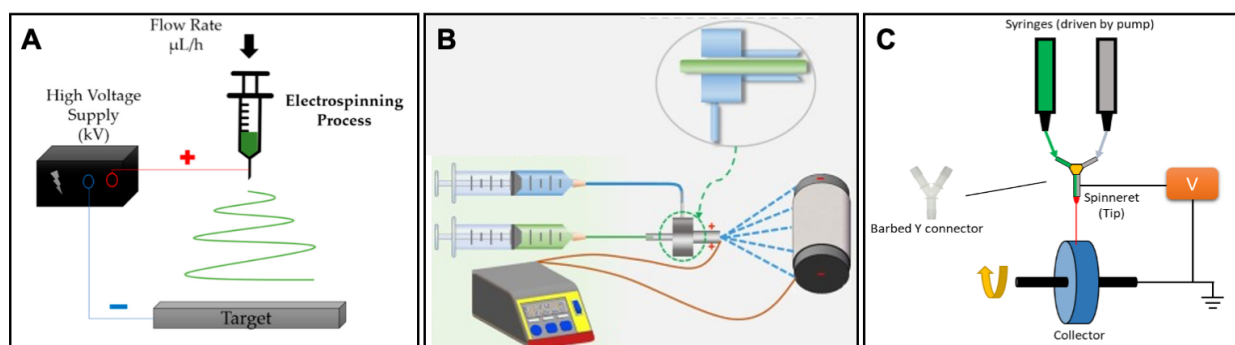
Figure 2. Diagram depicting electrospinning apparatus. Blend electrospinning and emulsion electrospinning (**A**) (reprinted from Ref. [68], open access, Copyright© 2023 by the authors, licensee MDPI), coaxial electrospinning (**B**) (reprinted with permission from Ref. [69] Copyright© 2023 Elsevier), and side-by-side electrospinning (**C**) (reprinted from Ref. [70], open access, Copyright© 2019 by the authors, licensee MDPI).

For pure chitosan, the electrospinnability is restricted by the strong intramolecular hydrogen bonding and the sparse entanglement of chains during electrospinning. Due to the polycationic nature of chitosan in solution, a rigid chemical structure is formed [71]. Methods exist to enhance the spinnability of chitosan, such as employing highly acidic excipient concentrations to decrease the surface tension of the chitosan solution, a critical factor in electrospinning. However, high acid concentrations present drawbacks such as eco-unfriendliness and cytotoxicity in vitro, leading to a reduction in the applicability of the resulting nanofibers in tissue engineering [72]. The second method is to increase the spinnability by mixing chitosan with other polymers, e.g., PEO, PCL, polyurethan (PU), PLA, and PVA. These co-electrospun polymers can be mixed into a single fluid prior to electrospinning or while electrospinning. Table 1 summarizes electrospinning approaches in the preparation of chitosan nanomembranes for various applications. The chitosan solution is blended with co-spinning polymers to improve spinnability. A third solution is to modify chitosan and use the resulting chitosan derivatives to develop this solution.

Table 1. Electrospinning techniques, co-spinning agents, and applications of chitosan-based electrospun nanofibers.

Techniques	Co-Spinning Agents	Applications	Ref.
Uniaxial electrospinning (Blend electrospinning)	PEO	Air filtration	[45]
		Food packaging	[73–75]
		Biomedical/pharmaceutical products	[76–78]
	PEO/tea tree oil liposomes	Food packaging	[79]

Table 1. *Cont.*

Techniques	Co-Spinning Agents	Applications	Ref.
	PEO/bromelain liposomes	Wound dressing	[80]
	PEO/gelatin	Wound dressing	[81]
	PEO/melittin	Acne treatment	[82]
	PEO/platelet-derived growth factor	Wound dressing	[83]
	PEO/Pluronic® F-127/ Hydroxyapatite	Wound dressing	[84]
	PEO/urushiol	Antibacterial membrane	[85]
	PCL	Wound dressing, separation membrane	[86,87]
	PCL/chlorogenic acid-loaded halloysite nanotube	Food packaging	[88]
	PCL/pectin	Wound dressing	[89]
	PU	Air filtration	[90]
	PU/carbon nanotubes	Cardiac tissue engineering	[91]
	PLA	Food packaging	[92]
	PLA/SiO$_2$	Air filtration	[93]
	PLA/cinnamon essential oil	Food packaging	[94]
	PLA/PCL/gelatin	Tissue engineering	[95]
	PVA	Antibacterial membrane	[96]
		Air filtration	[97]
	PVA/indocyanine green	Wound dressing	[98]
	PVA/sodium silicate	Separation membrane	[99]
	PVA/collagen/Fe$_3$O$_4$	Antibacterial membrane	[100]
	PVA/baicalin liposomes	Food packaging	[46]
	PVA/PVP	Separation membrane, medical purpose	[101,102]
	PVA/gelatin	Wound dressing	[103]
	PVA [a]	Air filtration	[104]
		Food packaging, wound dressing	[105,106]
	PVA [a]/tea tree oil	Food packaging	[107]
	Collagen and fibroin	Wound dressing	[108]
	Kefiran	Tissue engineering	[109]
	Pectin/cyclodextrin/curcumin	Biomedical products	[110]
	Gum Arabic/anthocyanins	Food packaging	[111]
	Oleamide	Culture medium of C1 gas utilizing microorganism	[112]
Emulsion electrospinning			
	PCL	Wound dressing	[64,65]
	PCL/alginate [b]	Bone tissue engineering	[113]
	PCL/PVA	Wound dressing	[114]
	PVA	Cosmetics and pharmaceuticals	[115]
	PVA/aloe vera	Wound dressing	[116]
	PVA [b]	Wound dressing	[117]
	PLA	Periodontal tissue engineering	[118]
	PLA	Drug delivery	[119]
	Poly(hydroxyalkanoate)/cellulose	Separation membrane	[120]
Coaxial electrospinning			
	PEO	Bone tissue engineering	[53,66]
		Surgical antimicrobial membrane	[121]
		Drug delivery/controlled drug release	[122,123]
	PEO [b]	Controlled drug release	[51]
		Food packaging	[54]
	PCL	Separation membrane	[124]
		Controlled drug release	[52,125–129]
		Tissue engineering	[130,131]
		Controlled drug release	

Table 1. *Cont.*

Techniques	Co-Spinning Agents	Applications	Ref.
	PCL/PVA [b]	Controlled drug release	[50]
	PCL-Diol-b-PU [c]	Controlled drug release	[132]
	PLA	Controlled drug release	[47]
	PLLA	Patch graft in carotid endarterectomy	[133]
	PVA	Drug delivery/controlled drug release	[134–136]
	PVA [b,d]	Drug delivery	[137]
	PVA/PVP	Separation membrane	[138]
	Gelatin	Food packaging	[139]
	PU/gelatin	Wound dressing	[140]
	Cellulose	Anode materials for lithium-ion batteries	[141]
	Collagen/essential oils	Wound dressing	[142]
	Origanum minutiflorum oil	Biomedical products	[143]
	Extracellular matrix components	Articular cartilage tissue engineering	[144]

[a] Co-spinning with quaternary ammonium chitosan; [b] co-spinning with carboxymethyl chitosan; [c] co-spinning with poly(N-isopropylacrylamide)-grafted chitosan; [d] co-spinning with sodium carboxymethyl chitosan.

In a study by Chen et al. (2022) [72], chitosan electrospun fibers were prepared using 2% w/w acetic acid, 2% w/w succinic acid, and 5% w/w citric acid as solvents by blending chitosan with PVA to study the effects of various kinds of organic acids on the characteristics of nanofibers. Under a controlled condition (0.9 mm needle size, 0.4 mL/h spinning rate, 18 kV, room temperature, and 10 cm collection distance from the needle tip to the rotating collector), these low concentrations of organic acids provided good spinnability comparable to a high concentration of glacial acetic acid (80% v/v). The use of succinic acid and citric acid produced smaller-diameter nanofibers with average diameters of 337 and 324 nm, which were slightly smaller than the use of acetic acid (342 nm) [72]. Nanofiber mats produced by acetic acid or succinic acid were found to be flexible, white, and airy, but the mats produced using citric acid were rigid and fragile with fused morphology because of the higher boiling point of citric acid [72]. Moreover, suitable viscosity and conductivity of the polymer solution lead to efficient polymer stretching into continuous, uniform chitosan nanofibers that are related to the fiber diameter [145,146]. The smaller diameters produced when citric acid and succinic acid are used cause increased conductivity and a lower viscosity of the polymeric solution, leading to a single jet dividing into multiple filaments as a result of heightened repulsion forces during the spinning process [145,146].

An increase in solubility by chitosan derivatization is another approach to enhancing the spinnability of chitosan. To enhance solubility and improve rheological properties, oxidation resistance, and thermal stability, the chitosan structure is chemically modified on the hydroxyl groups at the C3 and C6 positions, the amino group at C2, or both amino and hydroxyl groups. These modifications result in the formation of O-, N-, or N,O-modified chitosan derivatives [147]. For instance, quaternary ammonium chitosan, or N-(2-hydroxyl-3-trimethylammonium) propyl chitosan chloride (HTCC), is a type of chitosan derivative characterized by the presence of quaternary ammonium groups [148]. This chitosan derivative has higher water solubility and possesses higher antibacterial [104] and antiviral [149] activities compared to chitosan in its original form. Therefore, membranes containing HTCC nanofibers are appealing for various applications in which antibacterial [104,105] and antiviral [150,151] properties are in high demand.

HTCC synthesized from chitosan and 2,3-epoxypropyl trimethyl ammonium chloride and blended with PVA using water as a solvent was studied by Wang et al. (2019) [104]. The HTCC/PVA solution was spun through a metallic needle with an inner diameter of 0.86 mm and a feed rate of 0.656 mL/h under an electric potential fixed at 16.45 kV. The collection distance was 14 cm on the grounded metal plate encased in aluminum foil. The

electrospun nanofiber membranes comprising HTCC/PVA had diameters ranging from 300 to 400 nm [104]. Increasing the electrospinning voltage to 25 kV resulted in a reduction of the fiber diameter to 240 nm [106]. However, increasing the voltage beyond the critical value resulted in the bead formation of HTCC/PVA fibers [106]. The occurrence of beaded nanofibers at elevated voltages was linked to the reduction in the size of the Taylor cone and the simultaneous increase in jet velocity under consistent flow rates [58]. The pore size of the fibrous membrane increased with increasing HTCC concentrations. With increased HTCC content, the thermal stability of the nanofiber membrane also improved due to intermolecular and intramolecular hydrogen bonding in the HTCC/PVA structure; hence, the nanofiber was more stable. The PVA/HTCC nanofibers decomposed at ~360 °C, while the neat PVA nanofibers decomposed at ~315 °C [104]. The antimicrobial efficacy of the HTCC/PVA membrane surpassed that of the chitosan/PVA membrane. Specifically, when the mass ratio of HTCC/PVA was 4:6, the membrane exhibited antibacterial activity against Staphylococcus aureus and Escherichia coli, achieving about 99% inhibition [104]. However, the significant hydrophilicity of PVA/HTCC nanofibers impedes their application in aqueous environments. This challenge can be overcome by crosslinking [105]. Blend electrospinning was used to fabricate HTCC/PVA nanofiber membranes, followed by crosslinking with blocked diisocyanate (BI) to enhance water stability [105]. The electrospinning condition was fixed at 25 °C using a 21-gauge needle size, a 1.2 mL/h polymer solution feed rate, a 15.8 cm distance from the nozzle tip to the collector, and a 15 kV electric potential. The composite nanofibers were collected on polyethylene terephthalate (PET) fabric attached to a ground steel drum. The average diameter of crosslinked fibers was about 216 nm. The decrease in diameter of PVA/HTCC/BI nanofibers, compared with the non-crosslinked fibers, was attributed to the reduced viscosity of the polymer solution following the addition of BI. Moreover, higher BI content enhanced the water resistance and mechanical properties of the crosslinked nanofibers. Additionally, the thermal stability of the crosslinked PVA/HTCC nanofibers was improved to 431.82 °C [105].

Besides electrospinning using a blended solution passed through a single nozzle that produces a uniaxial fibrous membrane, more advanced multi-fluid electrospinning technologies have been developed. These methods enable the production of nanofibers with distinct properties, allowing for the creation of electrospun nanofiber membranes with a wide range of functionalities [152]. For instance, the use of core/shell nanofibers is compelling to enhance the properties of materials by combining the advantages of the core and the shell materials [64,65]. Moreover, sensitive active components or drugs can be protected in the core or both the core and shell [53,66]. The release behavior can then be controlled by the degradation of shell and core materials to release the active components [122,123]. In comparison, the active components incorporated into single fibers are distributed either within the fiber matrix or positioned near the surface of the fiber due to phase separation within the fiber. Therefore, the bioactivity of active components or biomolecules cannot be protected, and the release of the active components or biomolecules from such single-layer fibers is not controllable [122,123].

In a study by Deng et al. (2022) [53], an electrospun chitosan/PCL-guided bone regeneration (GBR) membrane having a core/shell structure loaded with simvastatin and calcium–phosphorus compounds in the core and shell, respectively, was developed. The calcium–phosphorus compounds in the core effectively enhanced swelling of the GBR membrane and enhanced in vitro mineralization ability. The sustained release of simvastatin loaded in the outer layer, containing multilayered materials of chitosan/PEO and PCL, was expected to be beneficial to the long-term bone generation process. Compared to the uniaxial pure PCL, there was no significant burst release of simvastatin, and the total cumulative release was lower [53]. This study demonstrates that incorporating chitosan into the shell layer can slow down the release rate of active components and prevent high local drug concentrations resulting from a burst release, which aligns with findings from other studies on the core/shell structure of chitosan composite nanofibers [52,123,128,137]. Appropriate selection of the shell and core materials is necessary to achieve the desired

release rate for a specific active component and an application. In the study by Ghasemvand et al. in 2023 [122], rosuvastatin, which has a beneficial effect on osteogenesis and the generation of new bone tissue, similar to simvastatin, was loaded in the core layer with chitosan/PEO, and PCL was used as the shell layer to enhance human mesenchymal stem cell osteogenesis. Utilizing the hydrophobic characteristics of PCL as a shell barrier while incorporating rosuvastatin into the core layer containing chitosan/PEO facilitated sustained release over 90 days with a lower initial release. These rosuvastatin-loaded nanofibers demonstrated improved proliferation and osteogenic differentiation of the stem cells [122]. Modifying the thickness or composition of the shell and core layers allows control over complex internal structures and drug release behavior. This capability can address the limitations of conventional electrospinning of chitosan in various biomedical applications, such as drug delivery and tissue engineering [153].

The primary limitation of traditional needle electrospinning is its low yield of chitosan fibers [154]. Needleless electrospinning was developed to enhance chitosan nanofiber production. In a study by Wang et al. (2016) [154], the production rate of composited chitosan nanofibers containing Ag and TiO_2 nanoparticles reached 50 g/h using needleless electrospinning, surpassing the 0.02–1 g/h achieved by the conventional single-needle electrospinning method. This needleless technique necessitates its own unique set of optimal parameters that differ from the needle process. Most of the experimental set-ups in needleless electrospinning of chitosan are based on the technology of Nanospider® using rotating spinnerets [154–158], as seen in Figure 3. Simultaneously, multiple Taylor cones and solution jets emerge on the surface of the rotating spinning electrode, which is submerged in a container filled with the polymeric solution. High voltages of 20–75 kV are applied as the chitosan and co-spinning solution volumes are increased to obtain higher productivity [154,155]. At low voltage levels, the volume of jet flow is lower compared to high voltage settings. Conversely, excessively high applied voltage can lead to electrical sparking, resulting in reduced productivity, discontinuous electrospinning [154], and the formation of beads [159]. In the recent publication by Mouro et al. (2023) [158], chitosan–PVA/PLLA nanofibers containing *Hypericum perforatum* L. extract were produced using emulsion electrospinning based on Nanospider®. The polymeric emulsion was prepared by homogenizing the chitosan–PVA aqueous solution and PLLA in chloroform/dimethylformamide (DMF). The electrospun fibers, in the absence of the herbal extract, exhibited uniform distribution and random orientation, with a mean diameter of 173 ± 41 nm. The addition of the extract reduced the viscosity of the electrospun solution, leading to a decrease in the average fiber diameter to approximately 120 nm. This approach was productive, but it required a higher voltage of 80 kv [158].
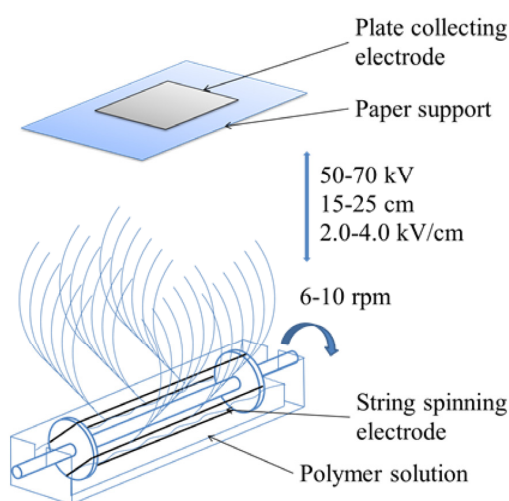
Figure 3. Example of a needleless electrospinning unit based on the technology of Nanospider® and process parameters (reprinted from Ref. [155], open access, Copyright© 2020 by the authors, licensee MDPI).

Despite the relatively high production rate of chitosan nanofibers, a few of them have been shown to be capable of producing chitosan nanofibers with a core/shell morphology. This is why this review focuses on needle-based electrospinning.

3. Emulsion Electrospinning

Emulsion electrospinning involves utilizing water-in-oil (W/O) or oil-in-water (O/W) emulsions with ordinary blend electrospinning equipment [114]. In electrospinning, the W/O type emulsion is typically utilized. Here, the polymer is dissolved in an oily solvent to generate an oil-phase solution, while chitosan is dissolved in an aqueous solution to produce a water-phase solution [113,114]. The method has been effectively employed for drug encapsulation within the core of nanofibers. Another benefit of emulsion electrospinning is its capability to produce nanofibers from diluted polymer solutions, enabling large-scale production of drug-loaded nanofibers [160]. Ensuring the stability of electrospinning emulsions is crucial. This stability can be achieved by incorporating surfactants such as Span 80 [113,118] and Tween 80 [114,120] as emulsifiers. The hydrophilic heads of surfactant molecules reside within the core, while the hydrophobic tails form an array in the shell. As a result of charge repulsion, the remaining surfactants migrate from the droplet phase to the outer surface, distributing themselves on the fiber surface with their hydrophilic groups facing the air [161]. Under the high voltage of the electrospinning process, the flow causes the dispersed droplets to move inward during the flow. This phenomenon results in the formation of the core of the fiber, while the continuous phase forms the shell [161]. After evaporation of the solvent, such as DMF/dichloromethane (DCM), nanofibers with core and shell structures are formed by water and oil phases, respectively [119]. The inclusion of the hydrophilic group enhances the surface wettability of the fibers. Thus, the emulsifier used in emulsion electrospinning can enhance the hydrophilicity of nanofibers produced from hydrophobic polymers [162]. Surfactants with electrostatic and hydrogen bonding effects can also influence nanofiber morphology [113,118]. The nanofiber size depends on concentrations of chitosan and co-electrospinning polymers as well as the spinning condition (Table 2).

Table 2. Emulsion electrospinning to prepare core/shell chitosan-based fibers with different co-spinning agents.

Emulsifier/ Stabilizer	Water Phase	Oil Phase	Condition	Fiber Diameter (nm)	Ref.
Span 80	Carboxymethyl chitosan and alginate (1:1) in distilled water	PCL	8 mm (syringe), 15 cm [b], 16 kV, 0.6 mL/h [c], 25 °C, 55% RH,	~2380	[113]
Span 80	Chitosan in 2% acetic acid (electrospinning on the surface of PLA fibers)	PLA emulsion (dissolved in chloroform)	0.838 mm [a], 15 cm [b], 17 kV, 0.012 mL/min [c]	About 200	[118]
Span 80	Chitosan (dissolved in 2% acetic acid)/PVP in DMF/DCM (3:7)	PLA	0.838 mm [a], 15 cm [b], 23 kV, 0.8 mL/h [c], 20 ± 2 °C, 25 ± 5% RH,	N/A	[119]
Tween 80	10% *w/v* PVA mixed with 4% *w/w* chitosan in 14% acetic acid	PCL solution (8% *w/v* in chloroform/DMF, 30:20) with addition of eugenol (5% *w/w* based on weight of PCL)	13 cm [b], 75.0 kV, 60 Hz, 25 °C, 35% RH	200–387 ± 179	[114]

Table 2. *Cont.*

Emulsifier/ Stabilizer	Water Phase	Oil Phase	Condition	Fiber Diameter (nm)	Ref.
Tween 80	Nanocellulose and 0.5% chitosan in pH 4 acetic acid	10% poly(hydroxylalkanoate) (dissolved in chloroform)	10 cm [b], 20 kV, 4 mL/h [c], 25.5 ± 0.5 °C, 55 ± 5% RH	N/A	[120]
Soybean lecithin	0.75% *w/v* chitosan in 0.75% *v/v* acetic acid	0.75% *w/v* PVA with addition of 7.5% *v/v Mentha piperita* essential oil, crosslinked by *w/v* sodium citrate	10 cm [b], 18 kV, 0.4 mL/min [c]	300–400	[115]
Sodium tripolyphosphate	5% aloe vera in PVA (10% *w/v*)/ 1% chitosan emulsion in 1% acetic acid)	10% *w/v* PVA	0.6 mm [a], 16.5 cm [b], 15 kV, 0.083 mL/min [c]	180–366	[116]
β-CD-citral inclusion complexparticles	Carboxymethyl chitosan/PVA	Citral	12 cm [b], 12 kV, 0.07 mL/min [c], 25 ± 5 °C, 50 ± 5% RH	268 ± 62	[117]
–	4% *w/w* chitosan in 90% acetic acid	10% *w/w* PCL in 3:1 chloroform/methanol	0.260 mm [a], 10 cm [b], 22 kV, 3 µL/min [c], room temperature,	413–3770	[64]
–	PCL/chitosan in formic acid/DCM	Formic acid/DCM by varying volume ratio of 7/3, 5/5 and 3/7 (*v/v*)	3.810 mm [a], 18 cm [b], 13 kV, 0.3 mL/h [c], 35 °C	143 ± 49	[65]

[a] Inner diameter of needle; [b] distance from needle tip to collector; [c] feeding rate.

The formation of electrospun fibers of two hydrophilic polymers, such as carboxymethyl chitosan and sodium alginate, is challenging due to their elevated surface tension and inadequate chain entanglement [113]. Therefore, the addition of an emulsifier, e.g., Span 80, to facilitate the dissolution of these two hydrophilic polymers in organic solvents for emulsion electrospinning is a way to fabricate fibers [113]. In a study by Tao et al. (2020) [113], core/shell fibers comprising carboxymethyl chitosan–sodium alginate/PCL were fabricated using emulsion electrospinning. The fibers were smooth and randomly oriented with a broad diameter range in microns (~2000 nm), which were much larger than the electrospun fibers in other studies (Table 2). It was reported that the inclusion of Span 80 led to an increase in the fiber diameter. Moreover, the swift evaporation of the organic solvent 1,1,1,3,3,3-hexafluoro-2-propanol used in this study diminished the stretching effect on the spinning fluid jet, leading to an enlargement in fiber diameter [113]. Compared to the use of chloroform/DMF, an organic solvent with lower volatility, the fiber diameter was about 10 times smaller (~200 nm) in the system of chitosan–PVA/PCL and Tween 80. However, the fibers displayed bead-on-a-string morphology [114].

Using the emulsion electrospinning approach, drugs or other active components located in the chitosan core layer are shielded from potential activity loss induced by external environmental factors and organic solvents [160]. Furthermore, the coating structure circumvents issues related to drug dispersion and abrupt release encountered in traditional electrospinning. Recent research indicates that nanofibers produced via emulsion electrospinning enhance the encapsulation efficiency, bioavailability, and stability of bioactive compounds while also improving barrier properties compared to conventional electrospinning techniques [163]. Zhang et al. (2023) [119] encapsulated a hydrophilic drug (such as Astragalus polysacharin) and a hydrophobic drug (such as camptothecin) into the chitosan core and PLA shell of nanofiber by emulsion electrospinning (Figure 4A,B). When Span 80 was used as an emulsifier, an increase in the volume ratio of the aqueous phase to the

organic phase in the W/O emulsion resulted in a reduction in the average diameter of the nanofibers. Under low concentrations of PLA, the nanofiber membranes exhibited a bead-in-string structure (Figure 4C). These membranes could serve as multi-drug carriers capable of loading drugs with varying solubilities [119]. In a study by Soon et al. (2019) [120], biocomposite nanofibers comprising poly(hydroxyalkanoate), nanocellulose, and chitosan were developed using pickering emulsion electrospinning. The pickering emulsion, stabilized by Tween 80, facilitated the formation of a homogeneous mixture of poly(hydroxyalkanoate), nanocellulose, and chitosan prior to electrospinning. Chitosan and nanocellulose were the colloidal particles for the W/O or O/W emulsion that rendered a stable and uniform emulsion. Poly(hydroxyalkanoate) in highly volatile chloroform crystallized more rapidly than nanocellulose and chitosan, resulting in the formation of a porous matrix that entrapped the adsorbents for Congo red removal. The poly(hydroxyalkanoate) nanofibers had less entangled straight fibers with micro-sized beads, resulting in weakened mechanical strength attributed to a decrease in intersection points among fibers [120]. After the incorporation of 2% *w/w* nanocellulose or 2% *w/w* chitosan, a high density of intersecting regions was found, resulting in better mechanical strength. However, when loading poly(hydroxyalkanoate) with 3% *w/w* nanocellulose and 1% *w/w* chitosan, the fibrous membrane had a high amount of irregular-shaped fillers linked together by thick poly(hydroxyalkanoate) fibers [120]. Pickering emulsion electrospinning was also proposed by Li et al. (2022) [117] to encapsulate high-loading citral, the highly volatile citrus essential oil. Citral served as the oil phase in the core, and a carboxymethyl chitosan/PVA solution was employed as the water phase in the shell. Cyclodextrin (CD) was also applied in the study. Because of the hydrophobic inner cavity, non-covalent complexes form between β-CD and lipophilic molecules like citral. The β-CD–citral inclusion complex was applied for stabilization of the O/W emulsion, and because of the interfacial area reduction of the O/W emulsion, particles of nanoscale or microscale spontaneously adhered to the interfaces of the emulsion. The resulting electrospun nanofibers, without citral loading, displayed a uniform and randomly distributed fiber structure with an average diameter of about 268 nm. After loading citral, the fiber diameters increased with the β-CD–citral complex, ranging from 1 to 10 μm. The increase in fiber size was caused by the increased viscosity of the emulsion. The instability of the jet was then reduced, leading to lower drawing forces and larger fiber diameters [117]. Similarly, Lamarra et al. (2023) [115] studied peppermint essential oil (Mentha piperita) encapsulation within nanostructures comprising chitosan, PVA, and soy lecithin. Soy lecithin was applied as a stabilizer by reducing interfacial tension between the oil and water phases in an O/W emulsion, adsorbing on the droplet surface, and inducing a negative surface charge to create repulsive forces that counteract destabilization [164]. The hydrophilic nature of both chitosan and PVA contributed to the hydrophilic characteristic observed in the O/W emulsion. However, the inclusion of essential oil and lecithin on the surface of the fibers rendered the electrospun material more hydrophobic. As the concentration of emulsion incorporated into the PVA matrix increased, an increasingly aligned pattern and reduced diameter of electrospun fibers were noted. The fibers exhibited diameters ranging between 300 and 400 nm [115]. The combined action of the essential oil and lecithin facilitated an increase in the elongation of the nanofibrous mat. This indicated a plasticizing effect from these components [115].

Some studies have concentrated on stable emulsion electrospinning without the use of surfactants. Without an emulsifier, emulsion can be formed by mixing two immiscible solutions, such as PCL and chitosan solutions [64,65]. PCL is wildly used as a biopolymer due to its good mechanical properties and biological compatibilities, but it has limited compatibility with hydrophilic polymers like chitosan. Thus, it can be used to form an emulsion with chitosan under high stirring conditions [64,65]. The different morphology (fiber size and mesh size) comprising chitosan in the core and PCL in the shell is linked to the melting and drying processes of PCL [64]. In a study by Ma et al. (2019) [65], a surfactant-free W/O emulsion system was prepared in immiscible formic acid/DCM as the solvent to obtain PCL/chitosan core/shell fibers by emulsion electrospinning at a

relative moderate electrospinning voltage of 13 kV (Figure 4D). Intact nanofibers were achieved by washing the shell with tetrahydrofuran. They found that the properties and morphologies of the fibers were altered by the polymer contents (Figure 4E–J). When increasing the chitosan content in the emulsion, the viscosity decreased, but the electrical conductivity increased. This generated a small fiber (diameter of 214 ± 90 nm) because the diameter of aqueous dispersed droplets increased. To prepare controllable core/shell-structured fiber by emulsion electrospinning, this work suggested that a component with electrical conductivity should be chosen as a core part [65]. Compared to the use of Span 80 as the emulsifier to prepare W/O emulsions of carboxymethyl chitosan/PCL and carboxymethyl chitosan/PCL/sodium alginate emulsion, the fiber diameters were 2.28 ± 1.23 and 2.38 ± 1.06 µm, respectively. Therefore, Span 80 significantly increases the spun fiber diameter [113].
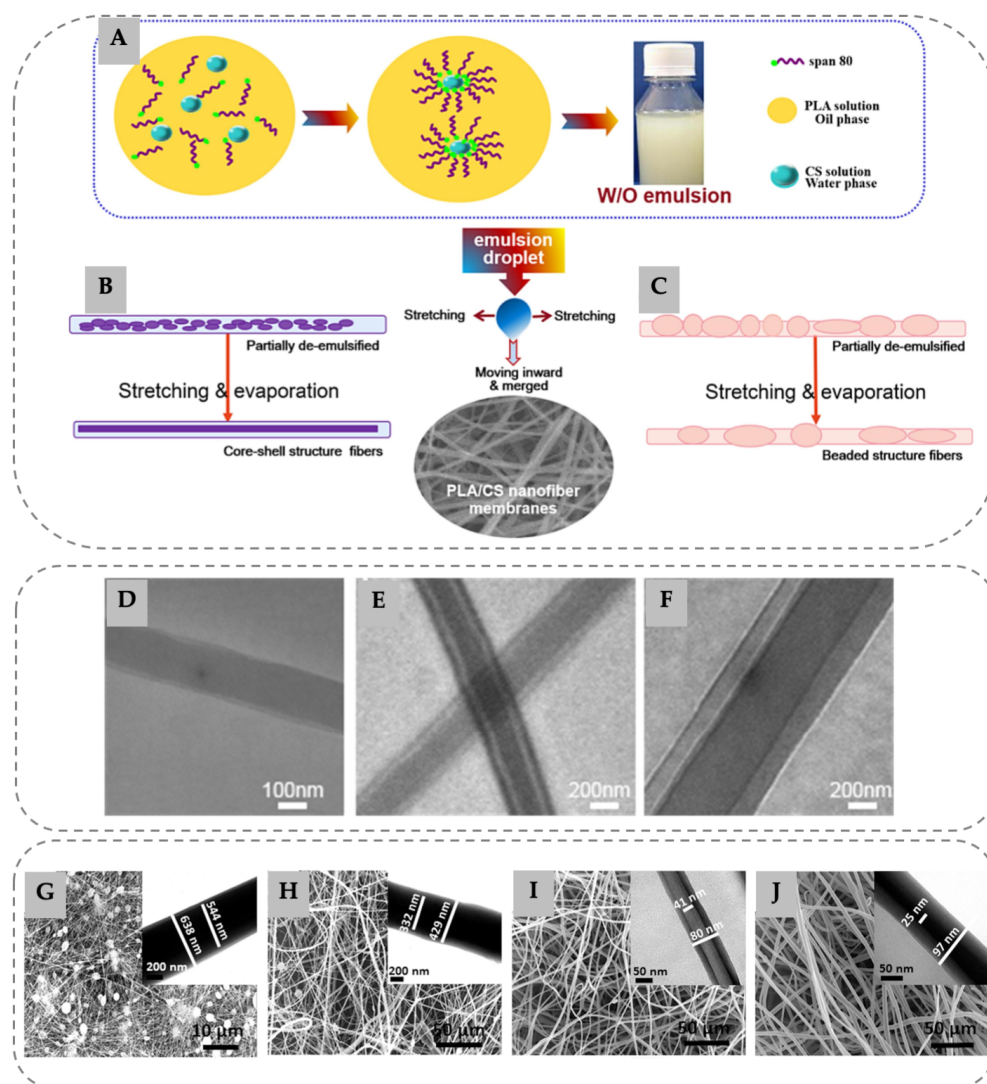
Figure 4. Emulsion electrospinning of chitosan-based nanofibers. Emulsion formation process (**A**); mechanism of core/shell fibers (**B**) and beaded-structure fibers (**C**) (reprinted with permission from Ref. [119], Copyright© 2023 Elsevier); and morphological appearances under transmission electron microscope (TEM) of nanofibers with different PCL/chitosan weight ratios of 6:2 (**D**), 8:2 (**E**), and 10:2 (**F**) dissolved in formic acid/DCM (reprinted with permission from Ref. [65], Copyright© 2019 Elsevier) and PCL/chitosan volume ratios of 1:2 (**G**), 1:1 (**H**), 2:1 (**I**), and 3:1 (**J**) when 10% *w/w* PCL in chloroform/methanol and 4% *w/w* chitosan in acetic acid were prepared and visualized by morphological appearances under a scanning electron microscope (SEM) (reprinted with permission from Ref. [64] Copyright© 2017 American Chemical Society).

4. Coaxial Electrospinning of Chitosan

Coaxial electrospinning is a technique to prepare nanofibers with a core/shell structure by generating coaxial jets from two immiscible liquids, unlike emulsion electrospinning, which relies on a single jet [165]. Nanofibers fabricated by coaxial electrospinning also show the potential to shield sensitive drugs or active components from harsh environments by loading in the core. The release of the active compounds is controlled by altering the shell thickness and polymer type. Due to its hydrophobic nature, PCL has been used to prepare core/shell nanofibers with chitosan in coaxial electrospinning. To increase biocompatibility for use as a scaffold in tissue engineering, a more biocompatible material is selected for use as the shell [165–167]. Therefore, the versatility of nanofibers as carrier materials in controlled and sustained delivery systems has been extensively studied to enhance therapeutic efficacy. Due to degradation through changes in mass and morphology, it is anticipated that these core/shell-structured fibers will demonstrate characteristics favorable for controlled delivery of drugs or other active components, as summarized in Table 3. The size of bead-free nanofibers depends on the flow rate settings. Table 3 illustrates that the average diameters of core/sheath nanofibers increase with higher inner and/or outer solution flow rates, while the inclusion of drugs into the polymer solution has minimal impact on fiber diameter. The marginal difference in fiber diameter observed in fibers incorporating the active compound may be due to the low concentration of the drug compared to that of the polymer [129]. A crucial requirement for forming the core/shell structure is the creation of a consistent two-component Taylor cone. If the core solution is not adequately integrated within the Taylor cone, the core/shell structure cannot be achieved [127]. Furthermore, a higher shell feed rate results in increased polymer content, leading to a larger Taylor cone and enhanced miscibility between the two solutions within the cone. This increase in Taylor cone size allows more time for the core solution to be in close proximity to the shell solution [127].

Table 3. Coaxial electrospinning to prepare core/shell chitosan-based fibers with different co-spinning agents and active components.

| Polymers in Core	Polymers in Shell	Active Components in Core	Condition	Fiber Diameter (nm)	Ref.
12% *w/v* PCL in trifluoroethanol	2% *w/v* chitosan in 1:1 *v/v* of 3% *w/v* acetic acid/ trifluoroethanol	Ciprofloxacin	0.92/1.64 mm orifice [a], 15 kV, 15 cm [b], 150–1000 rpm [c]	180–340 nm	[52]
13% *w/v* PCL in trifluoroethanol	4% *w/v* chitosan/PEO (8:2 *w/w*) in trifluoroacetic acid	Simvastatin (calcium phosphate in shell)	0.5/1.2 mm nozzle [a], room temperature, 30–40% RH, 23 kV, 15 cm	254.2 $\pm$ 34.5 nm core 103.6 $\pm$ 10.7 nm shell thickness	[53]
7:3 *w/w* chitosan/PEO in 1:1 *v/v* acetic acid	10% *w/v* PCL in 9:1 *v/v* chloroform/ DMF	Rosuvastatin	16–20 kV, 0.5 mL/h, 10–12 cm [b]	187–741 nm core 70 nm shell thickness	[122]
8% *w/v* cyclodextrin, 5% *w/w* triclosan, and 2% *w/w* PEO in 50% *v/v* acetic acid/water	3.5% *w/w* of chitosan and PEO (9:1) in 90% *v/v* acetic acid/ water	Triclosan loaded into cyclodextrin	0.514/1.372 mm orifice [a], 20 °C, 35% RH, 15–20 kV, 0.4–0.9 mL/h (shell), 0.3 mL/h (core), 20 cm [b], 100 rpm [c]	138–397 nm core 14–87 nm shell thickness	[123]

Polymers in Core	Polymers in Shell	Active Components in Core	Condition	Fiber Diameter (nm)	Ref.
8:2 of 5% *w/w* carboxymethyl chitosan/ 5% *w/w* PEO in water	10% *w/w* PU in DMF	Doxorubicin and folic acid incorporated into the UiO-66	0.635/1.27 mm orifice [a], 25 °C, 50% RH, 25 kV, 0.3–0.8 mL/h (shell), 0.5 mL/h (core), 15 cm [b], 200 rpm [c]	220–490 nm fiber diameter	[51]
8:2 of 4–6% *w/w* carboxymethyl chitosan/ 10% *w/w* PVA in water	8–12 *w/w* PCL in 80:20 *v/v* DCM:DMF	Doxorubicin loaded into nickel ferrite nanoparticles	0.635/1.27 mm orifice [a], 25 kV, 0.5 mL/h (core), 10–16.7 cm [b]	305–495 nm fiber diameter	[125]
12% *w/w* PCL in 70:30 *v/v* formic acid/ acetic acid	2:1–1:2 *v/v* of 12% *w/w* PCL and 12% *w/w* chitosan in 70:30 *v/v* formic acid/acetic acid	5FU and Fe_3O_4 nanoparticles	0.413/1.194 mm orifice [a], 15 kV, 0.08–0.1 mL/h (shell), 1.25–2 feeding ratio of shell/core, 14 cm [b], 200 rpm [c]	272–468 nm fiber diameter	[126]
2% *w/w* chitosan in 80% *v/v* acetic acid	15% *w/w* PCL in 90% *v/v* acetic acid	Tetracycline hydrochloride	0.4/1.7 mm orifice [a], 25 °C, 65% RH, 15 kV, 1 mL/h, 15 cm [b], 500 rpm [c]	285 ± 75 nm fiber diameter	[127]
6% *w/v* PCL in DCM	6% *w/v* chitosan in 80% *v/v* acetic acid	Rosuvastatin	0.35/1.1 mm orifice [a], 25 °C, 46% RH, 20 kV, 0.5 mL/h, 10 cm [b].	180–270 nm fiber diameter (120 nm core, 60 nm shell thickness)	[128]
2% *w/v* chitosan in 90% *v/v* acetic acid	15% *w/v* PCL in 1:1 *v/v* DCM/ ethanol	Resveratrol (ferulic acid in shell)	0.5/0.83 mm orifice [a], 24 °C, 68% RH, 25 kV, 0.4 mL/h (shell), 0.2 mL/h (core), 10–12 cm [b]	240 ± 50 nm	[129]
2:8 *v/v* of 5% *w/w* carboxymethyl chitosan and 10% *w/w* PVA	10% *w/w* PCL in 80:20 *v/v* DCM/DMF	Doxorubicin	0.21/1.6 mm orifice [a], 24 °C, 68% RH, 25 kV, 0.5 mL/h (shell), 0.5 mL/h (core), 12 cm [b], 1000 rpm [c]	410 nm	[50]
4% *w/v* polyvinyl pyrrolidone K90 and 12.5% *w/v* phospholipids in absolute ethanol	3.5% *w/v* carboxymethyl chitosan in 1:2 ethanol/water and 10% *w/v* in 1:1 ethanol/water	Carvedilol	0.413/1.067 mm orifice [a], 20 °C, 35% RH,12.5 kV, 0.4 mL/h (shell), 0.13 mL/h (core), 10 cm [b]	118–188 nm	[137]

[a] Inner diameter of needle; [b] distance from coaxial nozzle tip to collector; [c] speed of rotating collector.

Controlling the rotation speed of the collection drum allows for the production of both aligned and random core/shell fibers [52]. Cui et al. (2022) [52] studied PCL/chitosan core/shell nanofibrous membrane with both random and aligned fiber structures to facilitate a controlled release of ciprofloxacin, an antibacterial agent in healing wound infections, and to guide skin fibroblast arrangement (Figure 5). Various concentrations of ciprofloxacin were incorporated into the PCL solution to create different drug-loaded PCL/chitosan membranes. The prepared fibers possessed diameters ranging from 180 to 340 nm after

coaxial electrospinning using a nozzle (the inner diameters of the inner and outer tubes were 0.9 and 1.6 mm, respectively) operating at 15 kV, and the distance from the coaxial nozzle to the collector was set at 15 cm. Due to the elongation of the deposited fibers on the rapidly rotating collector, it was found that the aligned fibers exhibited a smaller diameter compared to the random ones. Their findings suggested that the PCL/chitosan membrane with aligned fibers loaded with 2% *w/w* ciprofloxacin having a diameter of about 230 nm with a 464 nm mesh size and 90% porosity showed antibacterial properties and biocompatibility to accelerate in vitro wound healing [52].
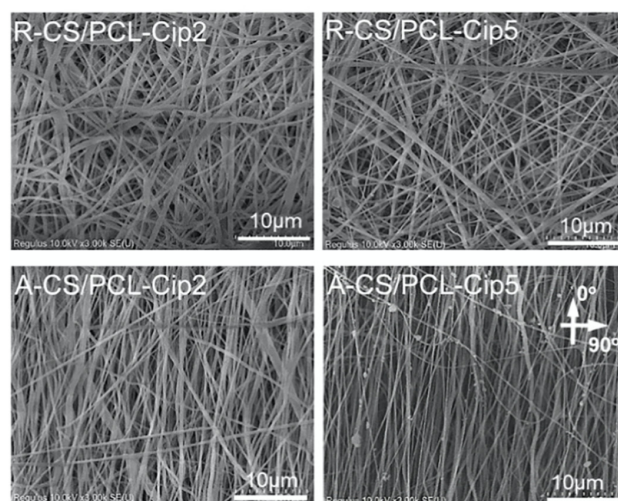

Figure 5. SEM images of random (R) and aligned (A) fiber structures of ciprofloxacin (cip)-encapsulated chitosan (CS)/PCL core/shell electrospun membranes prepared by coaxial electrospinning. Ciprofloxacin at concentrations of 2 and 5% *w/w* was loaded in the core with PCL. Controlling the rotation speed (ranging from 150 to 1000 rpm) of the collection drum allowed for the production of both aligned and random shell/core fibers (reprinted with permission from Ref. [52], Copyright© 2022 Elsevier).

A PCL/chitosan–PEO coaxial fibrous membrane crosslinked by fumigation with a 50% *w/w* glutaraldehyde having a core/shell structure with a shell thickness of 103 nm and a core diameter of 254 nm was obtained in [53]. Fibers that were smooth, round, and without beads were obtained using a coaxial electrospinning nozzle (inner diameters of inner and outer tubes were 0.5 and 1.2 mm, respectively) operating at room temperature under 30–40% humidity, 23 kV, and a distance from the coaxial nozzle to the collector of 15 cm. These findings are consistent with those reported in the study by Ma et al. (2019) [65]. In this study, the fabrication of PCL/chitosan core/shell nanofibers involved utilizing a stable emulsion system, yielding nanofibers with an average size within the range of 200 to 700 nm. However, inconsistent fibers and beads were present under emulsion electrospinning [65]. In the controlled release test of simvastatin loaded in the core to guide bone regeneration, the core/shell fibrous membranes exhibited a weight reduction of approximately 13% after three days, attributed to PEO dissolution. In comparison, the PCL uniaxial fibrous membrane showed minimal degradation yet released 45% of simvastatin within one day and approximately 80% after 14 days, without the protection of the shell layer [53]. In other words, a substantial release rate observed during the initial hours is commonly referred to as a burst release, a phenomenon documented in other studies [128].

For chitosan and PEO/PCL core/shell nanofibers with the loading of rosuvastatin, the shell thickness is thinner (ca. 70 nm), but the core sizes (187–741 nm) vary depending on the applied voltage (16–20 kV) and the distance from the coaxial nozzle to the collector (10–12 cm) [122]. On average, the fibers have a size of about 370 nm, with no micro- or nanoparticles present, confirming the formation of the core/shell structure. Ozkan et al. (2018) [168] reported a similar observation in coaxial chitosan/PCL nanofibers,

as inferred from TEM images. The chitosan core was covered by the PCL layer, with a distinct boundary observed between the core and shell materials [168]. For the release test, the burst release of rosuvastatin was found for chitosan and PEO membranes owing to the high dissolution rate of PEO and chitosan in phosphate-buffered saline (PBS) of pH 7.4 used as the releasing medium [122]. The drug was fully released within a 30-day period. In contrast to chitosan and PEO as a core with PCL as a shell, there was no rapid degradation observed in PBS. In addition, plasma treatment on this chitosan and PEO/PCL core/shell nanofiber mats enhanced the sustained release profile of rosuvastatin over 90 days. The plasma treatment acted as a barrier against rapid degradation, while the modified PCL enabled water penetration into the core [122]. On the other hand, for PCL/chitosan core/shell nanofibers with loading of rosuvastatin, the average diameter of the PCL core was approximately 120 nm, with the chitosan shell exhibiting a thickness of about 60 nm under coaxial electrospinning (inner diameters of inner and outer nozzle tubes were 0.35 and 1.1 mm, respectively) operating at room temperature, 46% humidity, 20 kV, and the distance from the coaxial nozzle to the collector of 1 cm [128]. In this study, chitosan was used as a shell material instead of PCL due to its hydrophilicity and its ability to enhance the biocompatibility of PCL. The pH-responsive nature of the chitosan shell led to an increase in the release of rosuvastatin as the pH value of the PBS solution decreased. For instance, approximately 22, 64, and 84% of rosuvastatin were released after 48 h for pH values of 7.4, 6, and 4, respectively [128].

Carboxymethyl chitosan, as a biocompatible pH-sensitive polymer, has been used in coaxial nanofibers for controlled delivery of anticancer drugs such as doxorubicin [51]. At physiological pH, the amine functional groups of carboxymethyl chitosan are not ionized, which impedes the diffusion of PBS into the nanofibers and prolongs the release of the drug. At an acidic pH, these functional groups are protonated, leading to an increase in electrostatic repulsion between the carboxymethyl chitosan chains, greater swelling of the carboxymethyl chitosan chains, and acceleration of the drug release from nanofibers [125]. The carboxymethyl chitosan can also chelate to the metal oxides, and carboxymethyl chitosan functionalized with magnetic ferrite nanoparticles has been used for targeted delivery of drugs [125]. To facilitate the electrospinning of carboxymethyl chitosan, blends of PVA and PEO have been incorporated into carboxymethyl chitosan solutions. The carboxymethyl chitosan cores are then coated with hydrophobic polymers, such as PCL and PU [50,51,125] (Figure 6). Abasalta et al. (2021) [125] studied the integration of doxorubicin into carboxymethyl chitosan–nickel ferrite nanoparticles/PCL core/shell nanofibers, aiming for controlled release of doxorubicin against MCF-7 breast cancer cells. Under optimal conditions of carboxymethyl chitosan and PCL concentrations of 4.9 and 9.6%, respectively, and an applied voltage-to-distance ratio of 2.1 kV/cm, thinner fibers with an average diameter of 300 nm were formed [125]. The fiber diameter was decreased from 460 and 360 to 280 nm as the PCL solution flow rate decreased from 0.8 and 0.5 to 0.3 mL/h, respectively [125]. This diameter range is similar to that in the study of doxorubicin/folic acid/UiO-66 nanoparticles loaded in carboxymethyl chitosan–PEO/PU core/shell nanofibers at the same shell flow rate [51]. Because of the reduced fiber diameter, the rate of drug release from the magnetic core/shell nanofibers exhibited a gradual decrease compared to that from the larger fibers and the carboxymethyl chitosan/PCL nanofibers alone [50]. This was because nickel ferrite nanoparticles filled in some pores, and the diffusion from the magnetic carboxymethyl chitosan matrix of the drug molecules was therefore difficult [125].
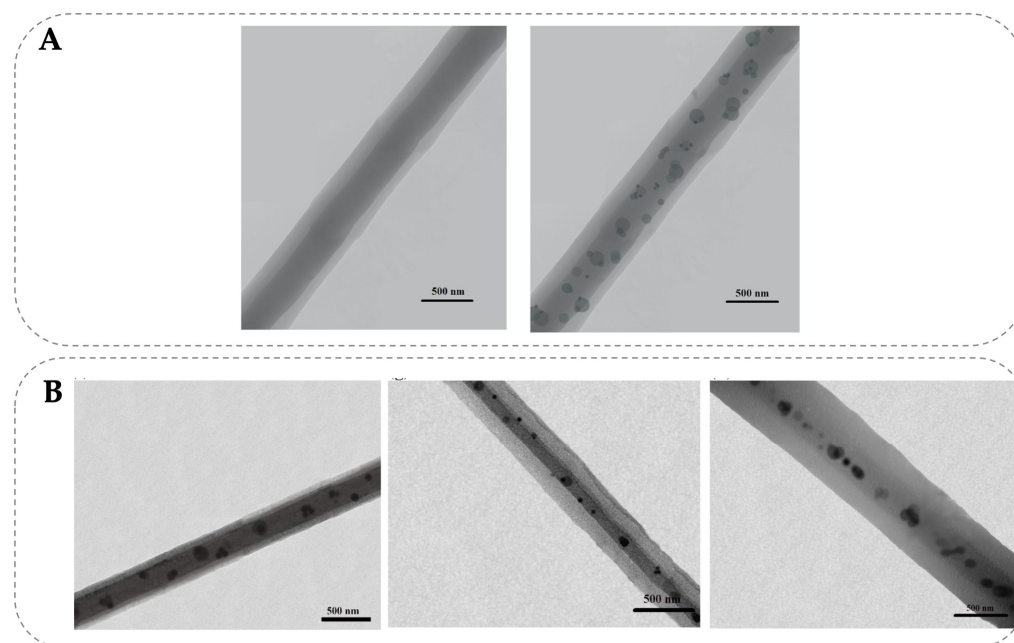
Figure 6. TEM images of core/shell chitosan electrospun nanofibers with drug-loaded metals in the core layer. Carboxymethyl chitosan/PEO/PU core/shell nanofibers (**A**) without (**left**) and with (**right**) loaded doxorubicin/folic acid/UiO-66 (reprinted with permission from Ref. [51], Copyright© 2020 Elsevier). TEM images of carboxymethyl chitosan/PCL core/shell nanofibers loaded with doxorubicin/nickel ferrite (**B**) prepared at shell flow rates of 0.3 (**left**), 0.5 (**middle**), and 0.8 (**right**) mL/h (reprinted with permission from Ref. [125], Copyright© 2021 Elsevier).

The use of inclusion complexes of active compounds and CD before incorporation in electrospun fibers to provide a high loading efficiency and prolonged release has been studied [123]. Inclusion complexation has been proven to be an effective method for enhancing the bioavailability and aqueous solubility of non-water-soluble active compounds. A derivative of CD, such as β-CD, which has a lipophilic cavity to host nonpolar molecules, can be used as a complex with tea tree essential oil [107]. The tea tree essential oil serves as a natural preservative in foods, but it is highly volatile and cannot exert long-term antioxidant and antibacterial effects. Complexation with β-CD can reduce the evaporation of tea tree essential oil in nanofiber electrospinning with HTCC and PVA (Figure 7A) [107]. Hydroxypropylated derivative of γ-CD or hydroxypropyl-γ-CD has higher aqueous solubility compared to β-CD and is used as a carrier matrix of curcumin in chitosan/pectin electrospun nanofibrous films (Figure 7B–D) [110]. The ultimate nanofibrous films have ∼89% curcumin loading efficiency and demonstrate a pH-responsive release profile of curcumin in pH 5.4 and 7.4 media, alongside their high swelling capability. However, an initial rapid release occurs during the initial 30 min due to the uniaxial fiber, followed by a sustained release until reaching a plateau after 2 days [110]. The burst release may occur due to the diffusion of curcumin near the surface of the fiber. The sustained release is attributed to the coating (shell), which prolongs the release time of the curcumin [135]. The core/shell nanofibers display sustained-release profiles for curcumin for >48 h based on graphene-g-β-CD/chitosan nanofiber [135]. In the study by Ouerghemmi et al. (2022) [123], the coaxial electrospinning of β-CD loaded with triclosan/chitosan–PEO nanofibers was studied (Figure 7E). The carboxylic groups of CD that were protonated in concentrated acetic acid did not interact with the ammonium groups of chitosan, leading to the prevention of the formation of a polyelectrolyte complex at the needle output. The formation of aggregates due to the polyelectrolyte complex could inhibit the stretching of the jet. A smaller diameter (274–325 nm) and more homogeneous diameter ranges of the core/shell nanofiber increased with higher flow rates of the inner and/or outer solutions. Raising the voltage to 20 kV resulted in heightened electrostatic charges on the surface, promoting

increased stretching of the jet and the production of thinner nanofibers [123]. For the release of tricosan, the burst effect was observed within the first 4 h for the monolithic nanofibers. The core/shell nanofibers with a small diameter (<300 nm) released about 40% of tricosan after 4 h. However, due to the inhomogeneous thickness, no direct correlation was observed between the release and the thickness of the shell [123].
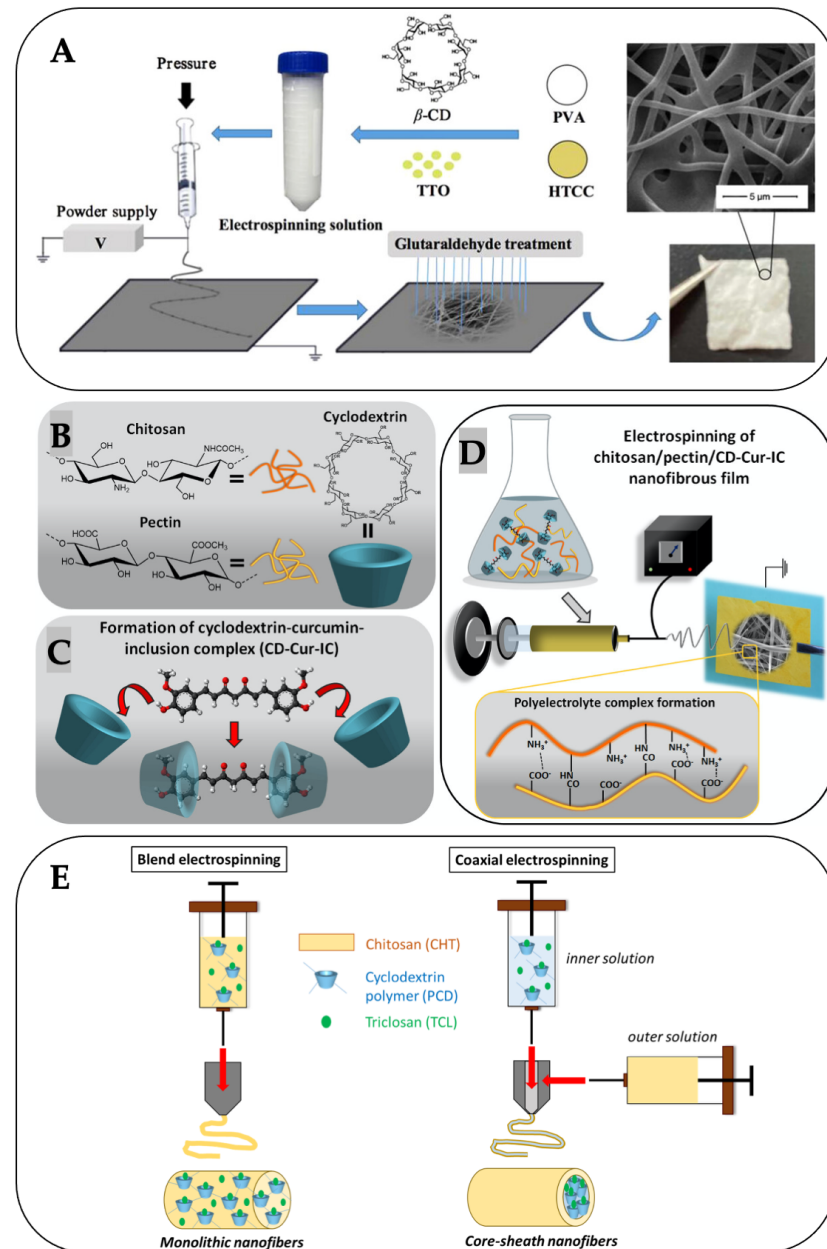
Figure 7. Illustration depicting the process of electrospinning nanofibers based on chitosan, cyclodextrin, and active components such as tea tree essential oil (TTO) (**A**) (reprinted with permission from Ref. [107], Copyright© 2023 Institute of Food Technologists and John Wiley & Sons, Inc.), curcumin (Cur) (**B**–**D**) (reprinted with permission from Ref. [110], Copyright© 2022 American Chemical Society), and triclosan (TCL) (**E**) (reprinted from Ref. [123], open access, Copyright© 2022 by the authors, licensee MDPI).
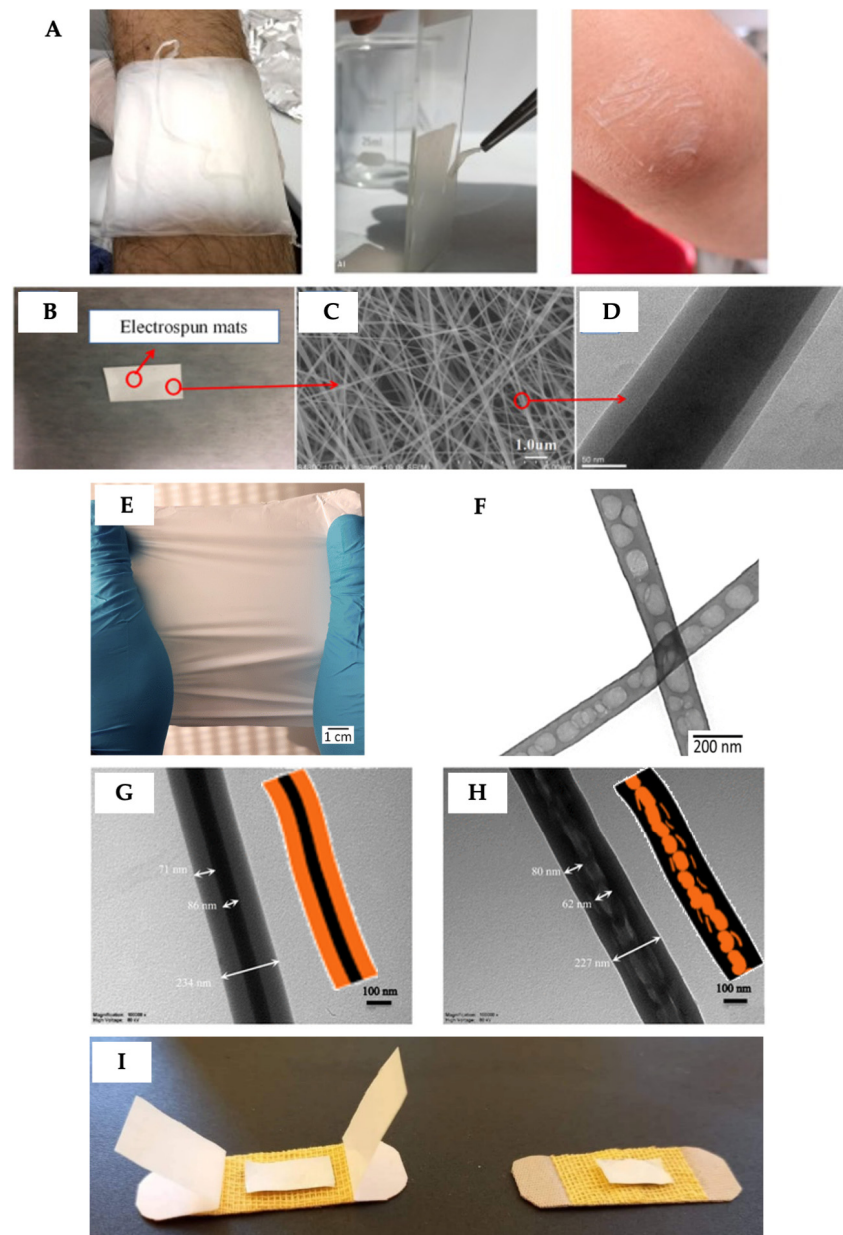
5. Applications

5.1. Textiles, Medical Dressings, and Scaffolds

The integration of nanomaterials into textiles has seen significant growth, largely owing to their customizable properties. This advancement has paved the way for the creation of smart textiles by incorporating nanomaterials with specific functionalities. Due to its antibacterial activity, high moisture absorption, and biodegradability, some textile products, e.g., sport apparel, pajamas, and underwear, that utilize chitosan blends have become readily available in the market, such as Craybon® (SWICOFIL AG) and Chitopoly® (Fuji-Spinning) [169]. Despite the availability of these commercial products for over a decade, research on the utilization of chitosan in textiles and fabrics continues, with ongoing investigations into methods like microencapsulation approaches [170]. In addition, chitosan is recognized in the field of wound management for its hydrating, hemostatic, and anti-inflammatory properties [76,171]. The acidic chitosan released from nanofibers aids in wound healing by reducing the pH of the wound environment [64]. This promotes cell adhesion [118] and stimulates cell proliferation and re-epithelialization to accelerate wound healing [172,173]. Therefore, chitosan and its derivatives have been electrospun and investigated for application in skin tissue engineering (Figure 8A) [174]. Chitosan-based nanofibers prepared by electrospinning have a suitable structure for fabricating dressings and scaffolds for regeneration of tissues including skin, nerves, blood vessels, bone, cartilage, tendon/ligament, and heart due to their fibrous, porous, nano-, and 3D structure, which is the same as the extracellular matrix [175,176]. A study has reported the invention of a portable electrostatic spinning device powered by batteries. This device is small, lightweight, and suitable for outdoor hemostasis [83]. The purpose is to prepare nanofibers that are closely attached to wounds, such as outdoor burns and scalds [83]. To enhance the wound-healing/tissue-engineering efficacy of neat chitosan nanofibrous wound dressing, hydroxyapatite (Figure 8B–D) [66,84], eggshell membrane [86], aloe vera [116], heparin [133], extracellular matrix proteins [144], collagen, and silk fibroin [108] are added to assist cell proliferation and accelerate wound healing compared to control gauze [108]. In addition, chitosan-based nanofibers fabricated with electrically conductive materials combined with exogenous electrical stimulation have been further studied to promote cellular activity [177].

Wound healing is a complex process that necessitates the use of suitable treatment products, which should be readily available and affordable. Currently, cheap and effective dressings for diabetic and nonhealing wounds are considered a clinical need to benefit patients and the economy [178]. A nanofibrous dressing should ideally have large pores, enabling the exchange of liquids and gases between the wound and its surroundings, yet be sufficiently small to block bacterial entry [179]. Enhanced antimicrobial wound dressings to improve the healing of infected wounds have been developed using electrospun chitosan/PVA by loading antimicrobial compounds such as indocyanine green [98], citric acid [72], *Hypericum perforatum* L. extract [114], citral from citrus essential oils [117], *Satureja mutica*, and *Oliveria decumbens* essential oils [180].

A binary antimicrobial core/shell nanofiber comprising nylon-6 in the core for mechanical stability and chitosan/PEO in the shell for bacteriostatic action was also studied by Keirouz et al. (2020) [121]. The core/shell structure consisted of two antimicrobial agents: 5-chloro-8-quinolinol in the chitosan shell and poly(hexanide) in the nylon-6 core (Figure 8E,F). This study showed the feasibility of incorporating two antimicrobial agents in a bilayer format with spatial control. The developed antimicrobial core/shell nanofiber demonstrated effectiveness in inhibiting both *Staphylococcus aureus* and *Pseudomonas aeruginosa*, which are common bacteria in surgical-site infections, for the entire 12 h, whereas the uniaxial nanofiber showed effective inhibition against *Pseudomonas aeruginosa*. The degradation of the electrospun mat was affected by the polymer matrix material into which the antimicrobial agents were incorporated. Due to variations in degradation rates that were dependent on polymer composition and fiber properties, direct comparison of

the antimicrobial activity of core/shell fibers with single-polymer–drug systems was not feasible [121].

Figure 8. Wound dressing applications of chitosan electrospun nanofibers. Chitosan/quaternized chitosan nanofibrous mats on different surfaces showing their adhesion properties (**A**) (reprinted with permission from Ref. [174], Copyright© 2022 Elsevier). Hydroxyapatite–gelatin/chitosan–PEO core/shell nanofiber mat (**B**) and its SEM (**C**) and TEM (**D**) images (reprinted with permission from Ref. [66], Copyright© 2018 Elsevier). Nylon-6/chitosan core/shell nanofiber mat (**E**) and TEM image showing the internal morphology of the nanofibers containing 5-chloro-8-quinolinol in the chitosan shell, and poly(hexanide) in nylon-6 core (**F**) (reprinted from Ref. [121], open access, Copyright© 2020 by the authors, licensee BioMed Central Ltd. as part of Springer Nature.). TEM images and schematic illustration of the core/shell chitosan nanofibers with *Origanum minutiflorum* oil loaded in the core (**G**) and the shell (**H**) (reprinted with permission from Ref. [143], Copyright© 2017 Springer–Verlag GmbH Germany, part of Springer Nature). Essential-oil-encapsulated collagen hydrolysate–chitosan core/shell nanofiber mat (**I**) (reprinted from Ref. [142], open access, Copyright© 2021 by the authors, licensee MDPI).

The antimicrobial agents also affect the degradation rate of core/shell nanofibrous wound dressings. Clarithromycin, a macrolide antibiotic, and zinc oxide nanoparticles, recognized for their antibacterial and anti-inflammatory attributes, were integrated into core/shell nanofibers composed of chitosan, gelatin, and PU by Abasalta et al. (2022) [140]. The core layer consisted of PU and clarithromycin, while the shell layer comprised chitosan, gelatin, and ZnO. This study showed that for nanofibers with and without clarithromycin, the degradation rate in PBS was the same, while it was enhanced by loading ZnO into the nanofibers. Clarithromycin and ZnO nanoparticles were released from the core/shell nanofibers within 5 days and 1 day, respectively. The nanofibers exhibited 100% bactericidal activity against both Escherichia coli and Staphylococcus aureus. Cell viability tests suggested that loading 0.5% *w/w* of ZnO nanoparticles and 2000 μM of clarithromycin was optimal for developing chitosan-based nanofibrous wound dressings [140]. Plant extracts, such as essential oils, are a promising replacement for synthetic drugs due to their anti-inflammatory, antioxidant, antibacterial, and antifungal properties. Chitosan-based nanofibers in which *Origanum minutiflorum* oil was separately loaded into the core and shell were prepared (Figure 8G,H, respectively) and compared with the uniaxial fibers in [143]. The nanofiber membrane containing the essential oil in the shell had more antibacterial activity against *Pseudomonas aeruginosa* and *Staphylococcus aureus* than that in the core after 24 h. This was because the active essential oil was more easily released into the environment from the shell layer. The core component exhibited slow dissolution or sustained-release behavior over a short duration. Thus, the nanofibers in which OM was loaded to the core showed lower antimicrobial efficiency against both types of bacteria compared to the uniaxial nanofibers loaded with essential oil [143]. Râpă et al. (2021) [142] encapsulated essential oils from dill (*Anethum graveolens* L.) and lemon balm (*Melissa officinalis* L.) into collagen hydrolysates derived from bovine tendons and rabbit skins. These were then blended with a chitosan solution to create coaxial nanofiber wound dressings (Figure 8I). They found that the blend of these two essential oils improved antimicrobial suppression against *Staphylococcus aureus*, *Enterococcus faecalis*, *Candida albicans*, *Candida glabrata*, *Salmonella typhimurium*, and *Aspergillus brasiliensis* [142].

Other medical materials with sustained drug release features of chitosan core/shell electrospun nanofibers are briefly summarized in Figure 9, such as the slower release rate of tetracycline hydrochloride [127] (Figure 9A), curcumin [47] (Figure 9B), and doxorubicin [50] (Figure 9C) from the core layer and the wound healing efficiency of resveratrol/ferulic acid-loaded chitosan/PCL core/shell nanofibrous scaffolds [129] (Figure 9D). The core/shell structure of nanofibers, which combines the properties of different materials, plays a significant role in protecting sensitive drugs due to the shell layer, mitigating burst release, and controlling the release behavior of both hydrophilic and hydrophobic drugs [119,127]. Moreover, the drug encapsulation efficiency of core/shell nanofibers is higher than that of composite uniaxial nanofibers [50,51]. The release of the drug from the core/shell nanofiber occurs in two stages: first, from the core layer to the shell layer, followed by the release from the shell layer into the blood flow. This extended-release mechanism is suitable for the delivery of anticancer drugs such as doxorubicin [50,51,125] and 5-fluorouracil [126] to kill cancer cells. Core/shell fibers of carboxymethyl chitosan–PVA/PCL have been studied as a pH-sensitive doxorubicin drug carrier for targeted delivery [50]. The presence of carboxylic and amine groups within carboxymethyl chitosan induced heightened swelling and accelerated release of doxorubicin from the nanofibers under acidic conditions (pH 5.5) compared to physiological pH (pH 7.4). About 80% of the doxorubicin was liberated from the core/shell nanofibers within 20 days at pH 7.4 and within 10 days at pH 5.5. The PCL hydrophobic shell layer provided more sustained release of the drug molecules compared to drug release from uniaxial composite nanofibers due to the lower degradation rate of core/shell nanofibers. For uniaxial nanofibers, 80% of the cumulative release level was reached after 11 and 3 days. The prolonged release of doxorubicin from the core/shell nanofibers resulted in enhanced cytotoxic effects against MCF-7 breast cancer cells compared to those observed with the

composite nanofibers. Using carboxymethyl chitosan–PVA/PCL core/shell fibers having 36.4 mg drug/g nanofiber (100 µg of doxorubicin, 97% drug loading efficiency), the maximum cytotoxicity of MCF-7 cells was 57% after 7 days of testing [50]. Simultaneous release of doxorubicin and nickel ferrite nanoparticles from carboxymethyl chitosan–PVA/PCL core/shell nanofibers (100 µg of doxorubicin, 92.5% drug loading efficiency) had a synergic effect on MCF-7 cell death (maximum cytotoxicity is 83%) after 7 days of testing under the presence of a magnetic field [125]. The use of nickel ferrite nanoparticles enhanced the hydrophilicity of nanofibers and pore filling, which resulted in slower release of the drug. Similarly, the drug release from the nanofibers showed pH-dependent profiles because carboxymethyl chitosan causes more swelling and doxorubicin has higher solubility in acidic pH. The sustained release of doxorubicin from carboxymethyl chitosan–PVA–nickel ferrite/PCL core/shell fibers was obtained over 25 days [125]. Similarly, 82% MCF-7 cell death was obtained after 7 days of testing when doxorubicin and folic acid incorporated into the UiO-66 metal organic framework (MOF) were released from carboxymethyl chitosan– PEO/PU core/shell nanofibers (1 mg of doxorubicin, 96% drug loading efficiency) [51]. After a 10-day testing period, a maximum of 87% MCF-7 cell death was observed, largely due to the slower degradation rate of the core/shell nanofibers, which can be attributed to the higher flow rate of PU in the shell. The continuous release of both doxorubicin and folic acid from the carboxymethyl chitosan-PEO/PU nanofibers was sustained over a span of 30 days [51].

Chitosan-based core/shell nanofibers have been developed for GBR to preserve alveolar bone volume and induce bone regeneration because of gum disease [118,134] and bone defects [66,113]. Zhu et al. (2023) [131] fabricated a core/shell PCL–chitosan/PVA GBR membrane containing different amounts of resveratrol grafted to the core with PVA. The in vitro release experiment for 15 days demonstrated a consistent release profile of resveratrol from the membranes. The developed GBR membrane loaded with 0.5 and 1% *w/v* resveratrol released the drug in a sustained and controlled manner (about 70% cumulative release), which induced osteogenic differentiation of pre-osteoblasts (MC3T3-E1 cells) in vitro. From in vivo bone regeneration in rats, newly formed bone tissues with ca. 82% of bone volume over total bone volume and 0.70 g/cm^3 of bone mineral density were generated in the defect sites after 12 weeks of post-implantation [131] (Figure 9E). Other studies have also investigated the drug delivery system for supporting osteogenesis in human mesenchymal stem cells (hMSCs). For example, the release of rosuvastatin loaded into the core of a chitosan–PEO/PCL core/shell nanofibrous membrane was studied in [122]. A burst release of rosuvastatin was found in the uniaxial chitosan–PEO membrane because of the rapid rate of dissolution of PEO and chitosan in PBS. In addition, the entire drug was released within a span of 30 days. Unlike the core/shell membrane, the degradation of the membrane and the drug release could be prolonged for the entire 90 days of the experiment, but only 5% of the drug was released after 10 days and 20% after 90 days. The plasma-treated PCL shell acted as a barrier, slowing down the degradation of the chitosan–PEO core, while the treated PCL allowed water to penetrate into the core. The rosuvastatin was completely released with a sustained profile for 90 days. This induced osteogenic differentiation of hMSCs in vitro, as indicated by the calcium content and alkaline phosphatase (ALP) activity after 14 and 21 days [122]. For platelet-rich fibrin-loaded chitosan/PCL–chitosan core/shell nanofibrous scaffold, mixing chitosan with PCL in the shell can enhance water penetration into the core [130]. The release rate of the platelet-rich fibrin from the nanofibrous scaffold was ca. 24% after 10 days. Calcium deposited on the surface and the value of ALP activity of platelet-rich fibrin-loaded chitosan/PCL–chitosan core/shell nanofibrous scaffold were 40.33 µg/scaffold and 81.97 U/L, respectively, after 14 days, confirming the osteogenesis of hMSCs in vitro [130]. A dual simvastatin and calcium phosphate-loaded PCL/chitosan–PEO core/shell fibrous membrane with glutaraldehyde crosslinking was proposed in [53]. The loaded simvastatin in the core of GRB membranes was sustainably released for about two months (50% cumulative release). The inclusion of calcium phosphate in the shell layer offered additional sites for mineralization

and synergistically interacted with simvastatin to enhance the osteogenic differentiation of MSCs in vitro. The maximum values of ALP activity, osteocalcin, vascular endothelial growth factor, and platelet–endothelial cell adhesion molecule of the dual-loaded PCL/chitosan–PEO core/shell fibrous membrane were about 40, 10, 0.2, and 17 ng/mL, respectively, after 14 days. In vivo intramuscular implantation experiments suggested that the sustained, long-term release of simvastatin subsequently promoted angiogenesis and maintained local microvascular networks [53].
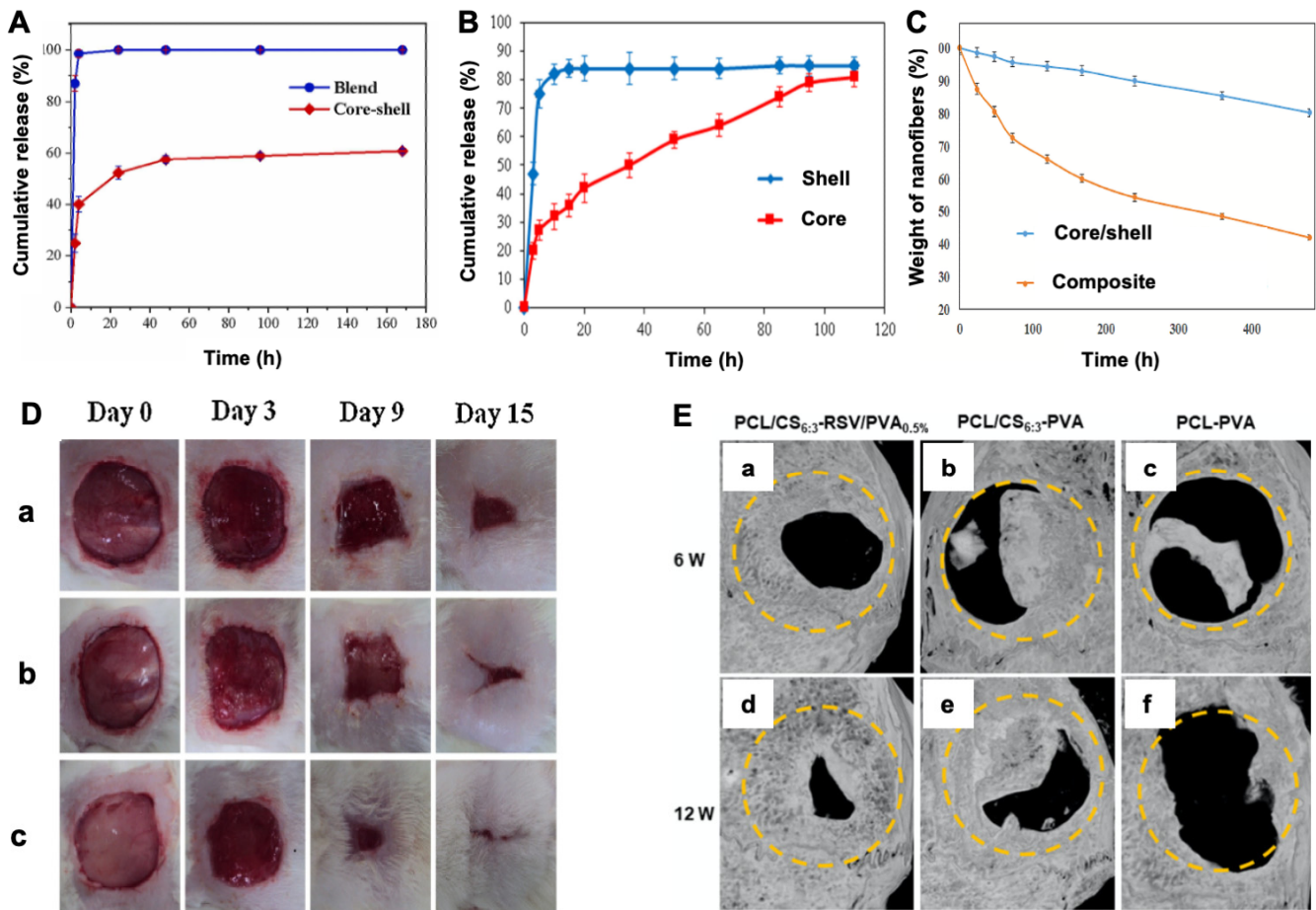
Figure 9. Drug delivery applications of chitosan core/shell electrospun nanofibers. Cumulative drug release of tetracycline hydrochloride from chitosan/PCL core/shell and blend nanofibers (**A**) (reprinted with permission from Ref. [127], Copyright© 2021 Elsevier). Release of curcumin from the electrospun PLA/chitosan core/shell nanofibers with curcumin in the core and shell layers (**B**) (reprinted with permission from Ref. [47], Copyright© 2019 Elsevier). Degradation rate of carboxymethyl chitosan/PVA/PCL/doxorubicin composite and core/shell nanofibers (**C**) (reprinted with permission from Ref. [50], Copyright© 2021 Elsevier). In vivo wound healing evaluation (**D**) after treatment with saline (a) chitosan/PCL (b), resveratrol/ferulic acid-loaded chitosan/PCL, and (c) nanofibrous scaffolds (reprinted with permission from Ref. [129], Copyright© 2016 Elsevier). In vitro cranial defect coverage (**E**) after treatment with PCL–chitosan/resveratrol–PVA (**a,d**), PCL–chitosan/PVA (**b,e**), and PCL/PVA (**c,f**) core/shell fibrous membranes (reprinted with permission from Ref. [131], Copyright© 2023 Elsevier).

5.2. Filtration Membranes/Absorbent

Filtration is a crucial process in various manufacturing industries, such as those involved in producing drinking water, pharmaceuticals, semiconductors, and air conditioning systems. It ensures that products meet quality standards and creates a pollution-free working environment [181]. Fibrous membrane systems offer superior adsorption capabilities compared to conventional powder- and bead-based systems [124]. Membrane separation is a potential technology for the highly efficient removal of organic and inorganic contaminants. Materials for the production of membranes include polyethylene (PE), polypropylene (PP), and PU for air filters; glass fibers, ion exchange resin, activated carbon, and ceramic for drinking water purification and wastewater treatment; and Teflon for hot gas filtration [181]. These filter materials are non-degradable, which means they carry some safety/environmental risks that can become a new environmental issue [182]. Therefore, greener alternatives to membranes should be used. The growing use of natural or renewable materials reflects a commitment to sustainability, prioritizing reuse and durability while minimizing harm to both people and the environment [99]. Therefore, the recent interest in the development of biopolymeric composites for environmental remediation applications is a key research area [87,183].

Chitosan-based biopolymers, rich in ionizable amino and hydroxyl groups, are adept at binding with negatively charged particles, thus augmenting filtration performance through electrostatic adsorption [87,101]. Electrostatic adsorption and Brownian diffusion are pivotal in filtering ultrafine particles (<0.3 μm), while interception and inertial impaction exert influence on larger particles (>0.3 μm) [23]. The filtration performance of fine particulate matter (PM) with a diameter ≤2.5 μm (PM 2.5) using the synergistic effect of electrospun chitosan/PEO nanofibers and porous MOF-5 was reported by Pan et al. (2022) [45]. Carboxyl groups were introduced to link amino groups on the chitosan nanofibers. Then, the functional carboxyl groups on the surface of the chitosan/PEO fibers were chemically bonded by binding Zn ions to encapsulate MOF-5 nanocrystals along the nanofiber direction. The multilayered nanofibrous structure of the electrospun membrane enhanced particle interception through Brownian diffusion. MOFs provided cavities and gas adsorption sites for the filter to remove PM 2.5 and strengthened the interactions between the membrane and PM. The electrospun nanofiber membrane composed of chitosan/PEO/MOF-5 exhibited a PM2.5 filtration efficiency of 99% and a quality factor of 0.0737 [45]. In addition, chitosan fibers serve as antimicrobial agents during the filtration process, reducing the deposition and emission of microorganisms and their byproducts. This helps prevent a decrease in filtration efficiency resulting from the degradation of filter media [90,93].

The functional groups of chitosan also provide a good adsorbent for heavy metals and dyes [101,120,124]. Water treatment and purification are of paramount importance due to the contamination of available water sources by toxic inorganic and organic chemicals, which pose a significant threat to human health and the environment. Electrospun cellulose acetate–PCL/chitosan core/shell nanofibers were applied for the removal of hexavalent chromium (Cr VI) from waste water [124]. Compared to the chitosan powder adsorbent, the core/shell-structured fibers possessed higher adsorption capability through the multilayer adsorption process (Freundlich isotherm model). With a core-to-shell ratio of 0.442, the cellulose acetate–PCL/chitosan fiber had a maximum adsorption capability of 126 mg/g at room temperature. These spun fibers also demonstrated excellent durability in acidic environments. After soaking in water for 48 h, virtually no loss was observed, and the adsorption capacity remained largely unchanged during five continuous cycles [124]. A chitosan/PVP/PVA hollow nanofiber membrane fabricated by coaxial electrospinning and applied for filtration of various organic dyes (malachite green, methylene blue, and crystal violet) and heavy metals (Cu^{2+}, Ni^{2+}, Cd^{2+}, and Pb^{2+}) was studied by Wu et al. (2023) [138]. Using the pre-crosslinked chitosan/PVP/PVA aqueous solution as the outer fluid and the PEO aqueous solution as the inner fluid, a PEO/chitosan, PVP, and PVA core/shell fibrous membrane was prepared and ultrasonicated in deionized water (Figure 10A). The PEO

core layer was subsequently eliminated to produce a hollow fiber membrane composed of CS/PVP/PVA nanofibers (Figure 10B). The hollow chitosan composite fibers, possessing a positive charge, repelled positive ions of heavy metals (Figure 10C) while allowing negative ions to permeate through the membrane. Additionally, they captured some ions within the membrane channel pores. The pollutants Cd^{2+} and Pb^{2+} and all the studied dyes were monolayer adsorbed on the nanofiber membrane surface according to the Langmuir model. For Cu^{2+} and Ni^{2+}, multilayer adsorption following the Freundlich model was found. The maximal adsorption capacities by the Langmuir model of Cu^{2+}, Ni^{2+}, Cd^{2+}, Pb^{2+}, malachite green, methylene blue, and crystal violet were 94, 9, 83, 77, 65, 54, and 43 mg/g, respectively.
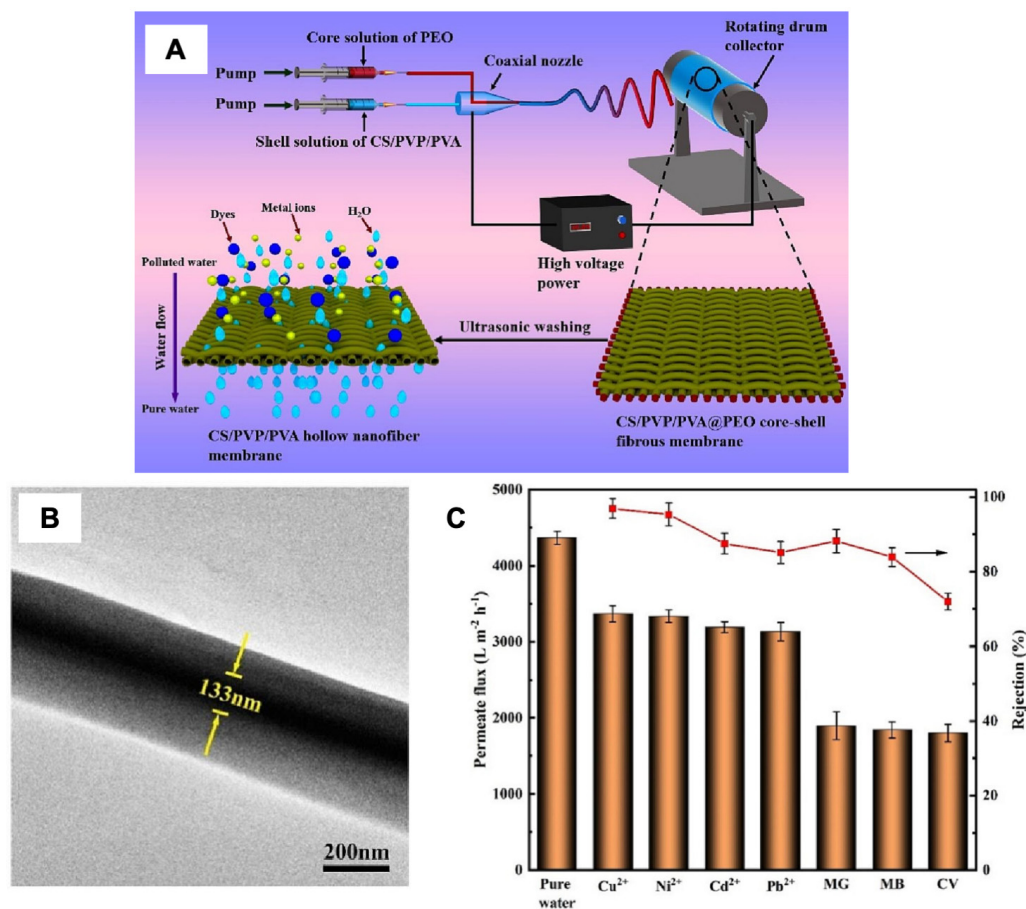

Figure 10. Filtration membrane application of chitosan core/shell electrospun nanofibers. Schematic illustration for the preparation (**A**), hollow fiber morphology (**B**), and permeate flux and rejection (**C**) of chitosan/PVP/PVA nanofiber membrane (MG: malachite green, MB: methylene blue, and CV: crystal violet; reprinted with permission from Ref. [138], Copyright© 2023 Elsevier).

5.3. Food Packaging

Foodborne diseases, foodborne pathogens, lipid oxidation, and inappropriate preservation during processing and storage cause food spoilage, food loss, and waste issues [184]. Synthetic preservatives, such as nitrate, nitrite, sulfite, organic acids, and bacteriocins, are often used to prolong the shelf life of food products, especially meat [185]. Food-grade polymers are selected for developing packaging films instead of using preservatives, which has the risk of drug residues and metabolic hindrance. Food packaging based on biopolymers such as chitosan to isolate food from the external environment is favored by consumers seeking healthy and safe food due to the non-toxicity and biodegradability of the biopolymer [186]. On the other hand, fabricating bilayer films with electrospun nanofibers or coating common polyethylene packaging films with chitosan nanofibers without reducing

the barrier or mechanical properties of the films have also been reported to modify the applications of electrospun nanofibers in food packaging [92]. Although chitosan provides good film-forming potential and antimicrobial properties, the inherent shortcomings of chitosan are its rapid dissolution in acidic aqueous solutions and its poor structural stability [187]. These make it difficult for chitosan-based materials to be used in environments with acidic agents [188]. In addition, the efficacy of chitosan against Gram-negative bacteria is comparatively lower in neutral environments compared to its effectiveness against Gram-positive bacteria. Various efforts have been undertaken to improve the acid resistance and antibacterial characteristics of chitosan nanofiber films, aiming to address these limitations for practical applications. For example, blending chitosan with other additives or crosslinking to minimize their disadvantages is a feasible strategy [187]. To improve its stability in acidic solutions, linear chitosan molecules are converted into network structures by crosslinkers, such as glutaraldehyde, glyoxal, epichlorohydrin, and ethylene glycol diglycidyl ether [76,77], and polybenzoxazine [189]. However, chemical crosslinkers are harmful to human cells and the environment. Physical or ionic crosslinking is a more promising method for preparing more biocompatible chitosan nanofiber membranes. To improve broad-spectrum antibacterial ability, some metals have been used as antibacterial agents. In addition, the mechanical properties of chitosan films are improved by the addition of metals such as SiO_2 [190], Ag_2O [191], Ag nanoparticles [192–194], ZnO [195], TiO_2 [141], and MoS_2 [196].

Currently, most research publications have focused on the fabrication of electrospun nanofibers by directly blending spinning solutions with bioactive compounds from plant extracts, such as chlorogenic acid from coffee [88], essential oil from tea trees [79,107], baicalin from skullcaps [46], and urushiol from lacquer trees [85]. These bioactive compounds contain phenolic compounds, e.g., polyphenols, terpenoids, and flavonoids, that have broad-spectrum antibacterial and antioxidant properties, resulting in increased food preservation [79,197]. Moreover, anthocyanins from plant extract can be used as color-changing indicators to monitor acid or alkaline released from microorganisms causing spoilage in fresh foods [111]. The technique of combining bioactive compounds has received attention for the development of effective and sustainable food preservation techniques because the biocompounds encapsulated in the nanofibers exhibit sustained release with enhanced antioxidant and antimicrobial activities in food packaging [79,197]. A blend of chitosan, PEO, and phenolic compounds was electrospun into a fiber film as food packaging. The phenolic compounds encapsulated in chitosan and PEO could enhance the antimicrobial properties against Gram-negative *Salmonella Typhimurium* and *Escherichia coli* and Gram-positive *Listeria innocua* and *Staphylococcus aureus* bacteria, which are all common bacteria involved in food contamination and spoilage [73,75]. This electrospun mat can prolong the shelf-life of fresh meat for one week [73,75]. The core/shell nanofibers with pullulan as a core layer and carboxymethyl chitosan/PEO as a shell layer were prepared by coaxial electrospinning and then loaded with carboxymethyl chitosan–nisin nanogels into the core layer of the nanofibers as antibacterial agents by Duan et al. (2023) [54] (Figure 11A–C). Pullulan and carboxymethyl chitosan were applied in the core and shell layers to increase the spinnability of the spinning solution. In addition, the carboxymethyl chitosan with the anionic group (–COO–) could self-assemble with positively charged nisin to form nanogels via electrostatic interactions, resulting in improving the stability of nisin. The nanogel-loaded nanofibers showed good mechanical properties and antibacterial activity against *Escherichia coli* and *Staphylococcus aureus*. During the test of bass fish storage, the core/shell electrospun chitosan nanofiber reduced lipid oxidation that produced rancid odor and delayed the growth of microorganisms, causing a reduction in the fish quality. The fresh bass fish packaged with the chitosan nanofiber film could be stored in a refrigerator at 4 °C for up to 15 days, while white slime and a fishy smell occurred in the unpackaged bass fish from the ninth day onwards [54].
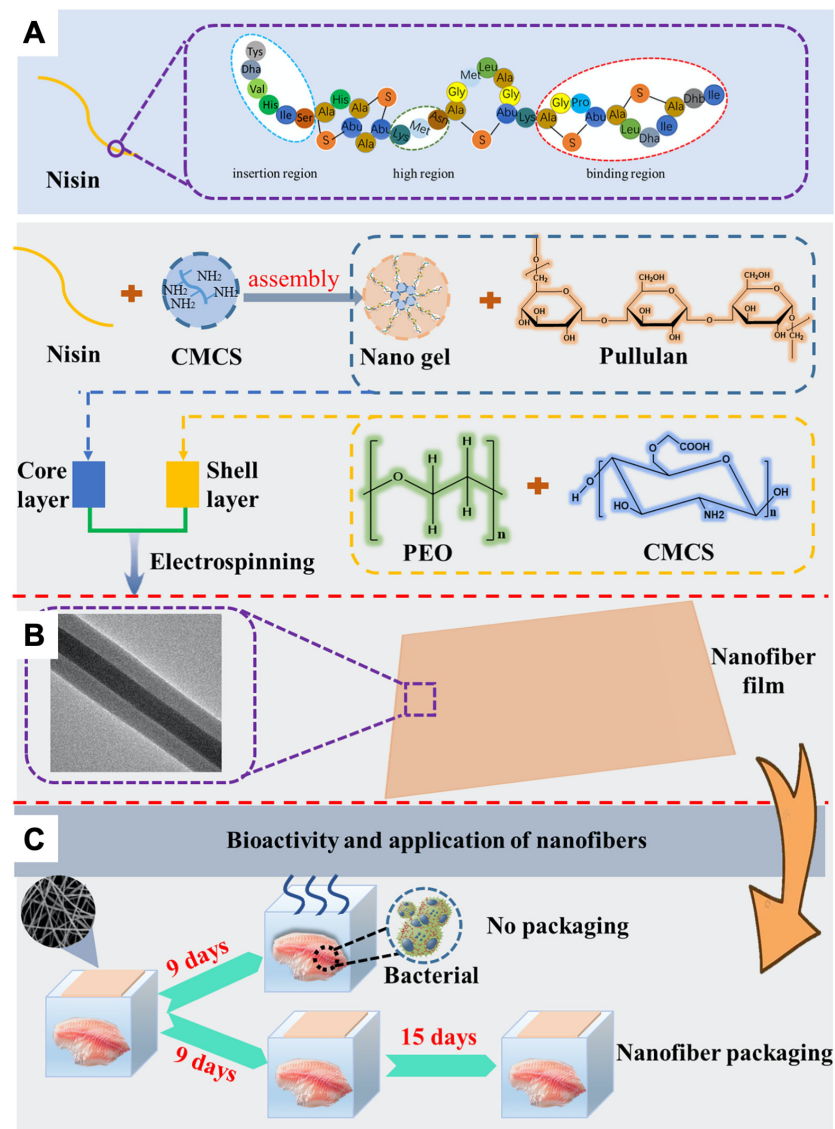
Figure 11. Food packaging application of chitosan core/shell electrospun nanofibers. Schematic illustration of the formation mechanism (**A**), core/shell morphology (**B**), and fresh bass fish packaging application (**C**) of pullulan/carboxymethyl chitosan–PEO core/shell nanofibers with nisin nanogel loading in the core (reprinted with permission from Ref. [54], Copyright© 2023 Elsevier).

6. Conclusions and Challenges

In the field of nanotechnology, the creation of nanostructures has been extensively investigated through the utilization of electrospinning techniques. Large-scale production of electrospun nanofibers is a relatively novel technology, and it seems to incur substantial costs. Among natural polymers that have a wide range of sources, the processability, biodegradability, and low-cost properties of chitosan mean it presents great potential as a bioactive material. It is already comprehensively implemented in various applications, especially for the replacement of plastics. The production cost of nanofibers can be reduced by the use of biopolymers like chitosan. Chitosan electrospun nanofibers with a core/shell nanostructure have been studied with the primary purposes of achieving a uniform structure in nanosize and facilitating the encapsulation of active compounds. Two electrospinning methods, emulsion electrospinning and coaxial electrospinning, are feasible approaches for the preparation of continuous nanofibers with a core/shell nanostructure. The difficulties in electrospinning chitosan are overcome by blending it with an easily

electrospinnable polymer, such as poly (ethylene oxide), polyvinyl alcohol, and other polymers described in this review. Continuous chitosan core/shell nanofibers with different properties can be obtained by modifying the spinning process parameters, altering the ratio of co-spinning polymers, and loading the active components to fit purposes including the use of biomaterials in biomedical/pharmaceutical applications, materials in environmental remediation, and food packaging.

Although the formation of core/shell chitosan-based nanofibers by emulsion electrospinning in a single emulsion has been reported, control over the thicknesses of the core and shell layers and fiber size is still challenging. Furthermore, the mechanism behind the formation of core/shell structures via emulsion electrospinning is complex, and there is a lack of specific studies regarding chitosan emulsion systems. In emulsion spinning solutions, the breakup of water or oil droplets in the solutions may not provide a core/shell structure due to the thermodynamic instability of the emulsion. Hence, stabilizers/surfactants are added to the formulation with organic solvents. Both stabilizers and organic solvents are hard to completely remove from the resulting nanofibers. The remaining stabilizers and organic solvents may cause biocompatibility and affect the biological activity of bioactive agents. Therefore, eliminating the need for emulsion stabilizers and organic solvents in the electrospinning process is a challenge.

Coaxial electrospinning of chitosan has been increasingly studied in recent years due to its simple technique but high ability to produce the core/shell morphology of chitosan nanofibers. Compared with conventional electrospinning, there are a higher number of parameters involved in producing optimal core/shell chitosan nanofibers. These include (i) physiochemical properties of the solvents for the core and shell solutions, which should be similar to avoid rapid polymer precipitation due to fast dissolution of the two solvents; (ii) high concentrations of chitosan and copolymers, leading to high viscosity that may cause needle clogging; and (iii) flow rates of the core and shell solutions that should be low and optimal. Due to low flow rates, the clear limitation of this method is its low productivity, particularly in the single Taylor cone-jet mode, where the spinneret orifice cannot produce more than one jet. To further refine this method, multi-needle electrospinning has been considered as a feasible approach to tackle this issue by increasing the number of needles to improve the production rate. However, besides needle clogging issues, this multiple-needle process has other major challenges, such as interference with the electrical fields generated by each needle, non-homogeneous fiber formation, bonding among fibers, and poor fiber distribution. Recently, more attention has been paid to developing needleless electrospinning techniques.

Chitosan-based nanofibers inherently display lower stability and mechanical properties in certain applications. For biomedical applications, the biomaterials are expected to have sufficient mechanical resistance to maintain their characteristics during application and support physiological loading. For environmental remediation applications, wastewater contains various corrosion agents that can dissolve chitosan nanofibrous membranes. Therefore, one of the approaches to resolving these challenges is crosslinking and/or modification/functionalization. These processes should be further investigated to gain better mechanical and anticorrosion properties for chitosan-based nanofibrous membranes. Nonetheless, the challenge persists in finding effective, environmentally friendly crosslinkers and establishing the ideal operating parameters for modification. Despite the feasibility of surface modification of nanofibers at the laboratory scale, scaling up these steps for mass production remains problematic.

Author Contributions: Conceptualization, S.T.; writing—original draft preparation, S.T. and T.C. writing—review and editing, S.T.; supervision, S.T. All authors have read and agreed to the published version of the manuscript.

Data Availability Statement: No new data were created.

Conflicts of Interest: The authors declare no conflicts of interest.

References

1. Xue, C.; Wilson, L.D. An Overview of the Design of Chitosan-Based Fiber Composite Materials. *J. Compos. Sci.* **2021**, *5*, 160. [CrossRef]
2. UN Environment Programme. Our Planet is Choking on Plastic. Available online: https://www.unep.org/interactives/beat-plastic-pollution/ (accessed on 29 November 2023).
3. OECD. Plastic Pollution is Growing Relentlessly as Waste Management and Recycling Fall Short, Says OECD. Available online: https://www.oecd.org/environment/plastic-pollution-is-growing-relentlessly-as-waste-management-and-recycling-fall-short.htm (accessed on 29 November 2023).
4. Lin, Z.; Chen, H.; Li, S.; Li, X.; Wang, J.; Xu, S. Electrospun Food Polysaccharides Loaded with Bioactive Compounds: Fabrication, Release, and Applications. *Polymers* **2023**, *15*, 2318. [CrossRef]
5. Hameed, A.Z.; Raj, S.A.; Kandasamy, J.; Baghdadi, M.A.; Shahzad, M.A. Chitosan: A Sustainable Material for Multifarious Applications. *Polymers* **2022**, *14*, 2335. [CrossRef]
6. Rashki, S.; Asgarpour, K.; Tarrahimofrad, H.; Hashemipour, M.; Ebrahimi, M.S.; Fathizadeh, H.; Khorshidi, A.; Khan, H.; Marzhoseyni, Z.; Salavati-Niasari, M.; et al. Chitosan-based nanoparticles against bacterial infections. *Carbohydr. Polym.* **2021**, *251*, 117108. [CrossRef] [PubMed]
7. Taokaew, S.; Kriangkrai, W. Chitinase-Assisted Bioconversion of Chitinous Waste for Development of Value-Added Chito-Oligosaccharides Products. *Biology* **2023**, *12*, 87. [CrossRef]
8. Rahimi, M.; Mir, S.M.; Baghban, R.; Charmi, G.; Plummer, C.M.; Shafiei-Irannejad, V.; Soleymani, J.; Pietrasik, J. Chitosan-based biomaterials for the treatment of bone disorders. *Int. J. Biol. Macromol.* **2022**, *215*, 346–367. [CrossRef] [PubMed]
9. Wang, N.; Ji, Y.; Zhu, Y.; Wu, X.; Mei, L.; Zhang, H.; Deng, J.; Wang, S. Antibacterial effect of chitosan and its derivative on Enterococcus faecalis associated with endodontic infection. *Exp. Ther. Med.* **2020**, *19*, 3805–3813. [CrossRef] [PubMed]
10. Malatjie, K.I.; Ndlovu, L.N.; Mishra, A.K.; Mishra, S.B. A Review on smart nanotextiles for filtration. *Nanotechnol. Environ. Eng.* **2023**, *8*, 449–459. [CrossRef]
11. Tien, N.D.; Lyngstadaas, S.P.; Mano, J.F.; Blaker, J.J.; Haugen, H.J. Recent Developments in Chitosan-Based Micro/Nanofibers for Sustainable Food Packaging, Smart Textiles, Cosmeceuticals, and Biomedical Applications. *Molecules* **2021**, *26*, 2683. [CrossRef]
12. Li, J.; Tian, X.; Hua, T.; Fu, J.; Koo, M.; Chan, W.; Poon, T. Chitosan Natural Polymer Material for Improving Antibacterial Properties of Textiles. *ACS Appl. Bio Mater.* **2021**, *4*, 4014–4038. [CrossRef]
13. Kalantari, K.; Afifi, A.M.; Jahangirian, H.; Webster, T.J. Biomedical applications of chitosan electrospun nanofibers as a green polymer—Review. *Carbohydr. Polym.* **2019**, *207*, 588–600. [CrossRef] [PubMed]
14. Mirbagheri, M.S.; Akhavan-Mahdavi, S.; Hasan, A.; Kharazmi, M.S.; Jafari, S.M. Chitosan-based electrospun nanofibers for diabetic foot ulcer management; recent advances. *Carbohydr. Polym.* **2023**, *313*, 120512. [CrossRef]
15. Biswal, A.; Purohit, S.S.; Swain, S.K. Chitosan based composite scaffolds in skin wound repair: A review. *J. Drug Deliv. Sci. Technol.* **2023**, *84*, 104549. [CrossRef]
16. Sánchez-Machado, D.I.; Maldonado-Cabrera, A.; López-Cervantes, J.; Maldonado-Cabrera, B.; Chávez-Almanza, A.F. Therapeutic effects of electrospun chitosan nanofibers on animal skin wounds: A systematic review and meta-analysis. *Int. J. Pharm. X* **2023**, *5*, 100175. [CrossRef] [PubMed]
17. Valachová, K.; El Meligy, M.A.; Šoltés, L. Hyaluronic acid and chitosan-based electrospun wound dressings: Problems and solutions. *Int. J. Biol. Macromol.* **2022**, *206*, 74–91. [CrossRef]
18. Chen, S.; Tian, H.; Mao, J.; Ma, F.; Zhang, M.; Chen, F.; Yang, P. Preparation and application of chitosan-based medical electrospun nanofibers. *Int. J. Biol. Macromol.* **2023**, *226*, 410–422. [CrossRef] [PubMed]
19. Vasudevan, A.; Tripathi, D.M.; Sundarrajan, S.; Venugopal, J.R.; Ramakrishna, S.; Kaur, S. Evolution of Electrospinning in Liver Tissue Engineering. *Biomimetics* **2022**, *7*, 149. [CrossRef]
20. Cui, C.; Sun, S.; Wu, S.; Chen, S.; Ma, J.; Zhou, F. Electrospun chitosan nanofibers for wound healing application. *Eng. Regen.* **2021**, *2*, 82–90. [CrossRef]
21. Khan, S.A.; Khan, S.B.; Kamal, T.; Asiri, A.M.; Akhtar, K. Recent Development of Chitosan Nanocomposites for Environmental Applications. *Recent Pat. Nanotechnol.* **2016**, *10*, 181–188. [CrossRef]
22. Anwar, Y. Antibacterial and lead ions adsorption characteristics of chitosan-manganese dioxide bionanocomposite. *Int. J. Biol. Macromol.* **2018**, *111*, 1140–1145. [CrossRef]
23. Shao, Z.; Chen, H.; Wang, Q.; Kang, G.; Wang, X.; Li, W.; Liu, Y.; Zheng, G. High-performance multifunctional electrospun fibrous air filter for personal protection: A review. *Sep. Purif. Technol.* **2022**, *302*, 122175. [CrossRef] [PubMed]
24. El-Aswar, E.I.; Ramadan, H.; Elkik, H.; Taha, A.G. A comprehensive review on preparation, functionalization and recent applications of nanofiber membranes in wastewater treatment. *J. Environ. Manag.* **2022**, *301*, 113908. [CrossRef] [PubMed]
25. Zhang, X.; Ru, Z.; Sun, Y.; Zhang, M.; Wang, J.; Ge, M.; Liu, H.; Wu, S.; Cao, C.; Ren, X.; et al. Recent advances in applications for air pollutants purification and perspectives of electrospun nanofibers. *J. Clean. Prod.* **2022**, *378*, 134567. [CrossRef]

26. Abdulhamid, M.A.; Muzamil, K. Recent progress on electrospun nanofibrous polymer membranes for water and air purification: A review. *Chemosphere* **2023**, *310*, 136886. [CrossRef]

27. Scaffaro, R.; Citarrella, M.C. Nanofibrous Polymeric Membranes for Air Filtration Application: A Review of Progress after the COVID-19 Pandemic. *Macromol. Mater. Eng.* **2023**, *308*, 2300072. [CrossRef]

28. Wang, H.; Qian, J.; Ding, F. Emerging Chitosan-Based Films for Food Packaging Applications. *J. Agric. Food Chem.* **2018**, *66*, 395–413. [CrossRef]

29. Kaya, M.; Khadem, S.; Cakmak, Y.S.; Mujtaba, M.; Ilk, S.; Akyuz, L.; Salaberria, A.M.; Labidi, J.; Abdulqadir, A.H.; Deligöz, E. Antioxidative and antimicrobial edible chitosan films blended with stem, leaf and seed extracts of Pistacia terebinthus for active food packaging. *RSC Adv.* **2018**, *8*, 3941–3950. [CrossRef]

30. Zhao, L.; Duan, G.; Zhang, G.; Yang, H.; He, S.; Jiang, S. Electrospun Functional Materials toward Food Packaging Applications: A Review. *Nanomaterials* **2020**, *10*, 150. [CrossRef]

31. Munteanu, B.S.; Vasile, C. Encapsulation of Natural Bioactive Compounds by Electrospinning—Applications in Food Storage and Safety. *Polymers* **2021**, *13*, 3771. [CrossRef]

32. Elamri, A.; Zdiri, K.; Bouzir, D.; Hamdaoui, M. Use of chitosan as antimicrobial, antiviral and antipollution agent in textile finishing. *Fibres Text.* **2022**, *29*, 51–70. [CrossRef]

33. Abourehab, M.A.S.; Pramanik, S.; Abdelgawad, M.A.; Abualsoud, B.M.; Kadi, A.; Ansari, M.J.; Deepak, A. Recent Advances of Chitosan Formulations in Biomedical Applications. *Int. J. Mol. Sci.* **2022**, *23*, 10975. [CrossRef]

34. Picos-Corrales, L.A.; Morales-Burgos, A.M.; Ruelas-Leyva, J.P.; Crini, G.; García-Armenta, E.; Jimenez-Lam, S.A.; Ayón-Reyna, L.E.; Rocha-Alonzo, F.; Calderón-Zamora, L.; Osuna-Martínez, U.; et al. Chitosan as an Outstanding Polysaccharide Improving Health-Commodities of Humans and Environmental Protection. *Polymers* **2023**, *15*, 526. [CrossRef]

35. Malik, S.; Sundarrajan, S.; Hussain, T.; Nazir, A.; Ayyoob, M.; Berto, F.; Ramakrishna, S. Sustainable nanofibers in tissue engineering and biomedical applications. *Mater. Des. Process. Commun.* **2021**, *3*, e202. [CrossRef]

36. Lauricella, M.; Succi, S.; Zussman, E.; Pisignano, D.; Yarin, A.L. Models of polymer solutions in electrified jets and solution blowing. *Rev. Mod. Phys.* **2020**, *92*, 035004. [CrossRef]

37. Abrishamkar, A.; Nilghaz, A.; Saadatmand, M.; Naeimirad, M.; de Mello, A.J. Microfluidic-assisted fiber production: Potentials, limitations, and prospects. *Biomicrofluidics* **2022**, *16*, 061504. [CrossRef]

38. Song, J.; Kim, M.; Lee, H. Recent Advances on Nanofiber Fabrications: Unconventional State-of-the-Art Spinning Techniques. *Polymers* **2020**, *12*, 1386. [CrossRef]

39. Rocha, J.; Araújo, J.C.; Fangueiro, R.; Ferreira, D.P. Wetspun Polymeric Fibrous Systems as Potential Scaffolds for Tendon and Ligament Repair, Healing and Regeneration. *Pharmaceutics* **2022**, *14*, 2526. [CrossRef]

40. Barhoum, A.; Pal, K.; Rahier, H.; Uludag, H.; Kim, I.S.; Bechelany, M. Nanofibers as new-generation materials: From spinning and nano-spinning fabrication techniques to emerging applications. *Appl. Mater. Today* **2019**, *17*, 1–35. [CrossRef]

41. Ye, P.; Guo, Q.; Zhang, Z.; Xu, Q. High-Speed Centrifugal Spinning Polymer Slip Mechanism and PEO/PVA Composite Fiber Preparation. *Nanomaterials* **2023**, *13*, 1277. [CrossRef] [PubMed]

42. Gholipour-Kanani, A.; Daneshi, P. A Review on Centrifugal and Electro-Centrifugal Spinning as New Methods of Nanofibers Fabrication. *J. Text. Polym.* **2022**, *10*, 41–55.

43. Wang, X.-X.; Yu, G.-F.; Zhang, J.; Yu, M.; Ramakrishna, S.; Long, Y.-Z. Conductive polymer ultrafine fibers via electrospinning: Preparation, physical properties and applications. *Prog. Mater. Sci.* **2021**, *115*, 100704. [CrossRef]

44. Negm, N.A.; Hefni, H.H.H.; Abd-Elaal, A.A.A.; Badr, E.A.; Abou Kana, M.T.H. Advancement on modification of chitosan biopolymer and its potential applications. *Int. J. Biol. Macromol.* **2020**, *152*, 681–702. [CrossRef] [PubMed]

45. Pan, W.; Wang, J.-P.; Sun, X.-B.; Wang, X.-X.; Jiang, J.-Y.; Zhang, Z.-G.; Li, P.; Qu, C.-H.; Long, Y.-Z.; Yu, G.-F. Ultra uniform metal−organic framework-5 loading along electrospun chitosan/polyethylene oxide membrane fibers for efficient PM2.5 removal. *J. Clean. Prod.* **2021**, *291*, 125270. [CrossRef]

46. Lu, S.; Tao, J.; Liu, X.; Wen, Z. Baicalin-liposomes loaded polyvinyl alcohol-chitosan electrospinning nanofibrous films: Characterization, antibacterial properties and preservation effects on mushrooms. *Food Chem.* **2022**, *371*, 131372. [CrossRef] [PubMed]

47. Afshar, S.; Rashedi, S.; Nazockdast, H.; Ghazalian, M. Preparation and characterization of electrospun poly(lactic acid)-chitosan core-shell nanofibers with a new solvent system. *Int. J. Biol. Macromol.* **2019**, *138*, 1130–1137. [CrossRef]

48. Su, S.; Bedir, T.; Kalkandelen, C.; Ozan Başar, A.; Turkoğlu Şaşmazel, H.; Bulent Ustundag, C.; Sengor, M.; Gunduz, O. Coaxial and emulsion electrospinning of extracted hyaluronic acid and keratin based nanofibers for wound healing applications. *Eur. Polym. J.* **2021**, *142*, 110158. [CrossRef]

49. Augustine, R.; Rehman, S.R.U.; Ahmed, R.; Zahid, A.A.; Sharifi, M.; Falahati, M.; Hasan, A. Electrospun chitosan membranes containing bioactive and therapeutic agents for enhanced wound healing. *Int. J. Biol. Macromol.* **2020**, *156*, 153–170. [CrossRef]

50. Abasalta, M.; Asefnejad, A.; Khorasani, M.T.; Saadatabadi, A.R.; Irani, M. Adsorption and sustained release of doxorubicin from N-carboxymethyl chitosan/polyvinyl alcohol/poly(ε-caprolactone) composite and core-shell nanofibers. *J. Drug Deliv. Sci. Technol.* **2022**, *67*, 102937. [CrossRef]

51. Farboudi, A.; Mahboobnia, K.; Chogan, F.; Karimi, M.; Askari, A.; Banihashem, S.; Davaran, S.; Irani, M. UiO-66 metal organic framework nanoparticles loaded carboxymethyl chitosan/poly ethylene oxide/polyurethane core-shell nanofibers for controlled release of doxorubicin and folic acid. *Int. J. Biol. Macromol.* **2020**, *150*, 178–188. [CrossRef]

52. Cui, C.; Sun, S.; Li, X.; Chen, S.; Wu, S.; Zhou, F.; Ma, J. Optimizing the chitosan-PCL based membranes with random/aligned fiber structure for controlled ciprofloxacin delivery and wound healing. *Int. J. Biol. Macromol.* **2022**, *205*, 500–510. [CrossRef]
53. Liu, C.; Deng, D.; Gao, J.; Jin, S.; Zuo, Y.; Li, Y.; Li, J. Construction and Properties of Simvastatin and Calcium Phosphate Dual-Loaded Coaxial Fibrous Membranes with Osteogenic and Angiogenic Functions. *J. Bionic Eng.* **2022**, *19*, 1645–1657. [CrossRef]
54. Duan, M.; Sun, J.; Yu, S.; Zhi, Z.; Pang, J.; Wu, C. Insights into electrospun pullulan-carboxymethyl chitosan/PEO core-shell nanofibers loaded with nanogels for food antibacterial packaging. *Int. J. Biol. Macromol.* **2023**, *233*, 123433. [CrossRef]
55. Al-Abduljabbar, A.; Farooq, I. Electrospun Polymer Nanofibers: Processing, Properties, and Applications. *Polymers* **2023**, *15*, 65. [CrossRef]
56. Nadaf, A.; Gupta, A.; Hasan, N.; Fauziya; Ahmad, S.; Kesharwani, P.; Ahmad, F.J. Recent update on electrospinning and electrospun nanofibers: Current trends and their applications. *RSC Adv.* **2022**, *12*, 23808–23828. [CrossRef] [PubMed]
57. Giaconia, M.A.; dos Passos Ramos, S.; Araújo, T.A.; de Almeida Cruz, M.; Renno, A.C.; Braga, A.R.C. Scaffold Production and Bone Tissue Healing Using Electrospinning: Trends and Gap of Knowledge. *Regen. Eng. Transl. Med.* **2022**, *8*, 506–522. [CrossRef]
58. Haider, A.; Haider, S.; Kang, I.-K. A comprehensive review summarizing the effect of electrospinning parameters and potential applications of nanofibers in biomedical and biotechnology. *Arab. J. Chem.* **2018**, *11*, 1165–1188. [CrossRef]
59. Guo, Y.; Wang, X.; Shen, Y.; Dong, K.; Shen, L.; Alzalab, A.A.A. Research progress, models and simulation of electrospinning technology: A review. *J. Mater. Sci.* **2022**, *57*, 58–104. [CrossRef]
60. Han, W.; Wang, L.; Li, Q.; Ma, B.; He, C.; Guo, X.; Nie, J.; Ma, G. A Review: Current Status and Emerging Developments on Natural Polymer-Based Electrospun Fibers. *Macromol. Rapid Commun.* **2022**, *43*, 2200456. [CrossRef]
61. Angel, N.; Li, S.; Yan, F.; Kong, L. Recent advances in electrospinning of nanofibers from bio-based carbohydrate polymers and their applications. *Trends Food Sci. Technol.* **2022**, *120*, 308–324. [CrossRef]
62. Ranganathan, S.; Balagangadharan, K.; Selvamurugan, N. Chitosan and gelatin-based electrospun fibers for bone tissue engineering. *Int. J. Biol. Macromol.* **2019**, *133*, 354–364. [CrossRef]
63. Wu, T.; Ding, M.; Shi, C.; Qiao, Y.; Wang, P.; Qiao, R.; Wang, X.; Zhong, J. Resorbable polymer electrospun nanofibers: History, shapes and application for tissue engineering. *Chin. Chem. Lett.* **2020**, *31*, 617–625. [CrossRef]
64. Pal, P.; Srivas, P.K.; Dadhich, P.; Das, B.; Maulik, D.; Dhara, S. Nano-/Microfibrous Cotton-Wool-Like 3D Scaffold with Core–Shell Architecture by Emulsion Electrospinning for Skin Tissue Regeneration. *ACS Biomater. Sci. Eng.* **2017**, *3*, 3563–3575. [CrossRef] [PubMed]
65. Ma, L.; Shi, X.; Zhang, X.; Li, L. Electrospinning of polycaprolacton/chitosan core-shell nanofibers by a stable emulsion system. *Colloids Surf. A Physicochem. Eng. Asp.* **2019**, *583*, 123956. [CrossRef]
66. Chen, P.; Liu, L.; Pan, J.; Mei, J.; Li, C.; Zheng, Y. Biomimetic composite scaffold of hydroxyapatite/gelatin-chitosan core-shell nanofibers for bone tissue engineering. *Mater. Sci. Eng. C* **2019**, *97*, 325–335. [CrossRef] [PubMed]
67. Abadi, B.; Goshtasbi, N.; Bolourian, S.; Tahsili, J.; Adeli-Sardou, M.; Forootanfar, H. Electrospun hybrid nanofibers: Fabrication, characterization, and biomedical applications. *Front. Bioeng. Biotechnol.* **2022**, *10*, 986975. [CrossRef] [PubMed]
68. Murillo, L.; Rivero, P.J.; Sandúa, X.; Pérez, G.; Palacio, J.F.; Rodríguez, R.J. Antifungal Activity of Chitosan/Poly(Ethylene Oxide) Blend Electrospun Polymeric Fiber Mat Doped with Metallic Silver Nanoparticles. *Polymers* **2023**, *15*, 3700. [CrossRef] [PubMed]
69. Wang, C.; Zhang, Q.; Hou, G.; Wang, C.; Yan, H. Sustained release of EGF/bFGF growth factors achieved by mussel-inspired core–shell nanofibers with hemostatic and anti-inflammatory effects for promoting wound healing. *Eur. Polym. J.* **2023**, *190*, 112003. [CrossRef]
70. Liu, W.; Zhang, J.; Liu, H. Conductive Bicomponent Fibers Containing Polyaniline Produced via Side-by-Side Electrospinning. *Polymers* **2019**, *11*, 954. [CrossRef]
71. Ignatova, M.; Manolova, N.; Rashkov, I. Electrospun Antibacterial Chitosan-Based Fibers. *Macromol. Biosci.* **2013**, *13*, 860–872. [CrossRef]
72. Chen, L.; Liu, Z.; Shi, J.; Wang, C.; Ding, L.; Ding, X.; Teng, G.; Wu, J.; Zhang, J. Preparation and antibacterial properties of chitosan/polyvinyl alcohol nanofibrous mats using different organic acids as solvents. *Process Biochem.* **2022**, *122*, 13–28. [CrossRef]
73. Arkoun, M.; Daigle, F.; Heuzey, M.-C.; Ajji, A. Antibacterial electrospun chitosan-based nanofibers: A bacterial membrane perforator. *Food Sci. Nutr.* **2017**, *5*, 865–874. [CrossRef] [PubMed]
74. Arkoun, M.; Daigle, F.; Heuzey, M.-C.; Ajji, A. Mechanism of Action of Electrospun Chitosan-Based Nanofibers against Meat Spoilage and Pathogenic Bacteria. *Molecules* **2017**, *22*, 585. [CrossRef] [PubMed]
75. Arkoun, M.; Daigle, F.; Holley, R.A.; Heuzey, M.C.; Ajji, A. Chitosan-based nanofibers as bioactive meat packaging materials. *Packag. Technol. Sci.* **2018**, *31*, 185–195. [CrossRef]
76. Dodero, A.; Brunengo, E.; Alloisio, M.; Sionkowska, A.; Vicini, S.; Castellano, M. Chitosan-based electrospun membranes: Effects of solution viscosity, coagulant and crosslinker. *Carbohydr. Polym.* **2020**, *235*, 115976. [CrossRef]
77. Dodero, A.; Scarfi, S.; Mirata, S.; Sionkowska, A.; Vicini, S.; Alloisio, M.; Castellano, M. Effect of Crosslinking Type on the Physical-Chemical Properties and Biocompatibility of Chitosan-Based Electrospun Membranes. *Polymers* **2021**, *13*, 831. [CrossRef]
78. Christ, H.-A.; Menzel, H. Electrospinning and Photocrosslinking of Highly Modified Fungal Chitosan. *Macromol. Mater. Eng.* **2023**, *308*, 2200430. [CrossRef]

79. Cui, H.; Bai, M.; Li, C.; Liu, R.; Lin, L. Fabrication of chitosan nanofibers containing tea tree oil liposomes against *Salmonella* spp. in chicken. *LWT* **2018**, *96*, 671–678. [CrossRef]

80. Bayat, S.; Amiri, N.; Pishavar, E.; Kalalinia, F.; Movaffagh, J.; Hashemi, M. Bromelain-loaded chitosan nanofibers prepared by electrospinning method for burn wound healing in animal models. *Life Sci.* **2019**, *229*, 57–66. [CrossRef]

81. Sun, C.; Yin, H.; He, J.; Zou, L.; Xu, Y. Fabrication and characterization of nanofibrous gelatin/chitosan-poly (ethylene oxide) membranes by electrospinning with acetic acid as solvent. *J. Polym. Res.* **2021**, *28*, 482. [CrossRef]

82. Rahnama, S.; Movaffagh, J.; Shahroodi, A.; Jirofti, N.; Fazly Bazzaz, B.S.; Beyraghdari, M.; Hashemi, M.; Kalalinia, F. Development and characterization of the electrospun melittin-loaded chitosan nanofibers for treatment of acne vulgaris in animal model. *J. Ind. Text.* **2022**, *52*, 15280837221112410. [CrossRef]

83. Sun, T.-C.; Yan, B.-Y.; Ning, X.-C.; Hui, C.; Xu, L.; Ding, Y.-N.; Yang, X.-L.; Ramakrishna, S.; Long, Y.-Z.; Zhang, J. Cool and hot chitosan/platelet-derived growth factor nanofibers for outdoors burns. *Int. J. Biol. Macromol.* **2022**, *218*, 409–419. [CrossRef]

84. Derakhshi, M.; Naseri, M.; Vafaeipour, Z.; Malaekeh-Nikouei, B.; Jafarian, A.H.; Ansari, L. Enhanced wound-healing efficacy of electrospun mesoporous hydroxyapatite nanoparticle-loaded chitosan nanofiber developed using pluronic F127. *Int. J. Biol. Macromol.* **2023**, *240*, 124427. [CrossRef]

85. Jie, X.; Shiu, B.-C.; Zhang, Y.; Wu, H.; Ye, Y.; Fang, R. Chitosan-Urushiol nanofiber membrane with enhanced acid resistance and broad-spectrum antibacterial activity. *Carbohydr. Polym.* **2023**, *312*, 120792. [CrossRef]

86. Guha Ray, P.; Pal, P.; Srivas, P.K.; Basak, P.; Roy, S.; Dhara, S. Surface Modification of Eggshell Membrane with Electrospun Chitosan/Polycaprolactone Nanofibers for Enhanced Dermal Wound Healing. *ACS Appl. Bio Mater.* **2018**, *1*, 985–998. [CrossRef] [PubMed]

87. Doan, H.N.; Vo, P.P.; Baggio, A.; Negoro, M.; Kinashi, K.; Fuse, Y.; Sakai, W.; Tsutsumi, N. Environmentally Friendly Chitosan-Modified Polycaprolactone Nanofiber/Nanonet Membrane for Controllable Oil/Water Separation. *ACS Appl. Polym. Mater.* **2021**, *3*, 3891–3901. [CrossRef]

88. Zou, Y.; Zhang, C.; Wang, P.; Zhang, Y.; Zhang, H. Electrospun chitosan/polycaprolactone nanofibers containing chlorogenic acid-loaded halloysite nanotube for active food packaging. *Carbohydr. Polym.* **2020**, *247*, 116711. [CrossRef] [PubMed]

89. Kaliaperumal, C.; Thulasisingh, A. In-vitro and in-vivo assessment of Polycaprolactone-Chitosan-Pectin imbibed nanofiber potentials as a wound healing biomaterial. *J. Polym. Res.* **2023**, *30*, 160. [CrossRef]

90. Mohraz, M.H.; Golbabaei, F.; Yu, I.J.; Mansournia, M.A.; Zadeh, A.S.; Dehghan, S.F. Preparation and optimization of multifunctional electrospun polyurethane/chitosan nanofibers for air pollution control applications. *Int. J. Environ. Sci. Technol.* **2019**, *16*, 681–694. [CrossRef]

91. Ahmadi, P.; Nazeri, N.; Derakhshan, M.A.; Ghanbari, H. Preparation and characterization of polyurethane/chitosan/CNT nanofibrous scaffold for cardiac tissue engineering. *Int. J. Biol. Macromol.* **2021**, *180*, 590–598. [CrossRef]

92. Dehghani, S.; Rezaei, K.; Hamishehkar, H.; Oromiehie, A. The effect of electrospun polylactic acid/chitosan nanofibers on the low density polyethylene/ploy lactic acid film as bilayer antibacterial active packaging films. *J. Food Process. Preserv.* **2022**, *46*, e15889. [CrossRef]

93. Zhu, M.; Xiong, R.; Huang, C. Bio-based and photocrosslinked electrospun antibacterial nanofibrous membranes for air filtration. *Carbohydr. Polym.* **2019**, *205*, 55–62. [CrossRef] [PubMed]

94. Liu, Y.; Wang, S.; Zhang, R.; Lan, W.; Qin, W. Development of Poly(lactic acid)/Chitosan Fibers Loaded with Essential Oil for Antimicrobial Applications. *Nanomaterials* **2017**, *7*, 194. [CrossRef] [PubMed]

95. Demina, T.S.; Bolbasov, E.N.; Peshkova, M.A.; Efremov, Y.M.; Bikmulina, P.Y.; Birdibekova, A.V.; Popyrina, T.N.; Kosheleva, N.V.; Tverdokhlebov, S.I.; Timashev, P.S.; et al. Electrospinning vs. Electro-Assisted Solution Blow Spinning for Fabrication of Fibrous Scaffolds for Tissue Engineering. *Polymers* **2022**, *14*, 5254. [CrossRef] [PubMed]

96. Galstyan, A.; Strokov, K. Influence of photosensitizer concentration and polymer composition on photoinduced antimicrobial activity of PVA- and PVA-chitosan-based electrospun nanomaterials cross-linked with tailor-made silicon(IV) phthalocyanine. *Photochem. Photobiol. Sci.* **2022**, *21*, 1387–1398. [CrossRef]

97. Sargazi, G.; Afzali, D.; Mostafavi, A.; Shadman, A.; Rezaee, B.; Zarrintaj, P.; Saeb, M.R.; Ramakrishna, S.; Mozafari, M. Chitosan/polyvinyl alcohol nanofibrous membranes: Towards green super-adsorbents for toxic gases. *Heliyon* **2019**, *5*, e01527. [CrossRef]

98. Qiu, H.; Zhu, S.; Pang, L.; Ma, J.; Liu, Y.; Du, L.; Wu, Y.; Jin, Y. ICG-loaded photodynamic chitosan/polyvinyl alcohol composite nanofibers: Anti-resistant bacterial effect and improved healing of infected wounds. *Int. J. Pharm.* **2020**, *588*, 119797. [CrossRef]

99. Mahatmanti, F.W.; Kusumastuti, E.; Wijayati, N. Electrospinning of nanofibers chitosan/PVA-sodium silicate. *J. Phys. Conf. Ser.* **2021**, *1918*, 032012. [CrossRef]

100. Abou-Okeil, A.; Refaei, R.; Khalil, E.M.; Moustafa, S.E.; Ibrahim, H.M. Fabrication of novel green magnetic electrospun nanofibers based on Fe_3O_4 nanoparticles/PVA/chitosan/collagen. *Egypt. J. Chem.* **2022**, *65*, 285–298. [CrossRef]

101. Wu, S.; Li, K.; Shi, W.; Cai, J. Preparation and performance evaluation of chitosan/polyvinylpyrrolidone/polyvinyl alcohol electrospun nanofiber membrane for heavy metal ions and organic pollutants removal. *Int. J. Biol. Macromol.* **2022**, *210*, 76–84. [CrossRef]

102. Bandatang, N.; Pongsomboon, S.-a.; Jumpapaeng, P.; Suwanakood, P.; Saengsuwan, S. Antimicrobial electrospun nanofiber mats of NaOH-hydrolyzed chitosan (HCS)/PVP/PVA incorporated with in-situ synthesized AgNPs: Fabrication, characterization, and antibacterial activity. *Int. J. Biol. Macromol.* **2021**, *190*, 585–600. [CrossRef] [PubMed]

103. Hadipour-Goudarzi, E.; Hemmatinejad, N.; Shokrgozar, M.A. Fabrication and DOE Optimization of Electrospun Chitosan/Gelatin/PVA Nanofibers for Skin Tissue Engineering. *Macromol. Mater. Eng.* **2023**, *308*, 2200562. [CrossRef]

104. Wang, C.; Fan, J.; Xu, R.; Zhang, L.; Zhong, S.; Wang, W.; Yu, D. Quaternary ammonium chitosan/polyvinyl alcohol composites prepared by electrospinning with high antibacterial properties and filtration efficiency. *J. Mater. Sci.* **2019**, *54*, 12522–12532. [CrossRef]

105. Wu, J.-Y.; Ooi, C.W.; Song, C.P.; Wang, C.-Y.; Liu, B.-L.; Lin, G.-Y.; Chiu, C.-Y.; Chang, Y.-K. Antibacterial efficacy of quaternized chitosan/poly (vinyl alcohol) nanofiber membrane crosslinked with blocked diisocyanate. *Carbohydr. Polym.* **2021**, *262*, 117910. [CrossRef] [PubMed]

106. Wu, J.-Y.; Wang, C.-Y.; Chen, K.-H.; Lai, Y.-R.; Chiu, C.-Y.; Lee, H.-C.; Chang, Y.-K. Electrospinning of Quaternized Chitosan-Poly(vinyl alcohol) Composite Nanofiber Membrane: Processing Optimization and Antibacterial Efficacy. *Membranes* **2022**, *12*, 332. [CrossRef] [PubMed]

107. Xia, Y.; Tang, X.; Wu, X.; Li, Y.; Xu, C.; Chen, S.; Wu, P. Electrospun chitosan-based nanofibers loading tea tree oil for fresh salmon fillet shelf-life extension. *J. Food Sci.* **2023**, *88*, 3075–3089. [CrossRef] [PubMed]

108. Yu, P.; Guo, J.; Li, J.; Shi, X.; Wang, L.; Chen, W.; Mo, X. Repair of skin defects with electrospun collagen/chitosan and fibroin/chitosan compound nanofiber scaffolds compared with gauze dressing. *J. Biomater. Tissue Eng.* **2017**, *7*, 386–392. [CrossRef]

109. Shokraei, S.; Mirzaei, E.; Shokraei, N.; Derakhshan, M.A.; Ghanbari, H.; Faridi-Majidi, R. Fabrication and characterization of chitosan/kefiran electrospun nanofibers for tissue engineering applications. *J. Appl. Polym. Sci.* **2021**, *138*, 50547. [CrossRef]

110. Celebioglu, A.; Saporito, A.F.; Uyar, T. Green Electrospinning of Chitosan/Pectin Nanofibrous Films by the Incorporation of Cyclodextrin/Curcumin Inclusion Complexes: pH-Responsive Release and Hydrogel Features. *ACS Sustain. Chem. Eng.* **2022**, *10*, 4758–4769. [CrossRef]

111. Shavisi, N.; Shahbazi, Y. Chitosan-gum Arabic nanofiber mats encapsulated with pH-sensitive Rosa damascena anthocyanins for freshness monitoring of chicken fillets. *Food Packag. Shelf Life* **2022**, *32*, 100827. [CrossRef]

112. Kang, E.; Moon, E.; Song, W.; Kim, L.H.; Hyung, J.S.; Jo, J.-H.; Park, J.-H.; Kim, M.-S.; Na, J.-G.; Choi, Y.S. Chitosan/oleamide nanofluid as a significant medium for enhancing gas utilization efficiency in C1-gas microbial biotransformation. *Chem. Eng. J.* **2022**, *433*, 133846. [CrossRef]

113. Tao, F.; Cheng, Y.; Tao, H.; Jin, L.; Wan, Z.; Dai, F.; Xiang, W.; Deng, H. Carboxymethyl chitosan/sodium alginate-based micron-fibers fabricated by emulsion electrospinning for periosteal tissue engineering. *Mater. Des.* **2020**, *194*, 108849. [CrossRef]

114. Mouro, C.; Simões, M.; Gouveia, I.C. Emulsion Electrospun Fiber Mats of PCL/PVA/Chitosan and Eugenol for Wound Dressing Applications. *Adv. Polym. Technol.* **2019**, *2019*, 9859506. [CrossRef]

115. Lamarra, J.; Rivero, S.; Pinotti, A.; Lopez, D. Nanofiber mats functionalized with Mentha piperita essential oil stabilized in a chitosan-based emulsion designed via an electrospinning technique. *Int. J. Biol. Macromol.* **2023**, *248*, 125980. [CrossRef] [PubMed]

116. Sosiati, H.; Nur Fatihah, W.; Yusmaniar, Y.; Nur Rahman, M.B. Characterization of the Properties of Electrospun Blended Hybrid Poly(Vinyl Alcohol)_Aloe Vera/Chitosan Nano-Emulsion Nanofibrous Membranes. *Key Eng. Mater.* **2019**, *792*, 74–79. [CrossRef]

117. Li, C.; Luo, X.; Li, L.; Cai, Y.; Kang, X.; Li, P. Carboxymethyl chitosan-based electrospun nanofibers with high citral-loading for potential anti-infection wound dressings. *Int. J. Biol. Macromol.* **2022**, *209*, 344–355. [CrossRef] [PubMed]

118. Shen, R.; Xu, W.; Xue, Y.; Chen, L.; Ye, H.; Zhong, E.; Ye, Z.; Gao, J.; Yan, Y. The use of chitosan/PLA nano-fibers by emulsion eletrospinning for periodontal tissue engineering. *Artif. Cells Nanomed. Biotechnol.* **2018**, *46*, 419–430. [CrossRef]

119. Zhang, W.; Liu, H.; Yan, L.; Mei, X.; Hou, Z. Combining emulsion electrospinning with surface functionalization to fabricate multistructural PLA/CS@ZIF-8 nanofiber membranes toward pH-responsive dual drug delivery. *Int. J. Biol. Macromol.* **2023**, *253*, 126506. [CrossRef] [PubMed]

120. Soon, C.Y.; Rahman, N.A.; Tee, Y.B.; Talib, R.A.; Tan, C.H.; Abdan, K.; Chan, E.W.C. Electrospun biocomposite: Nanocellulose and chitosan entrapped within a poly(hydroxyalkanoate) matrix for Congo red removal. *J. Mater. Res. Technol.* **2019**, *8*, 5091–5102. [CrossRef]

121. Keirouz, A.; Radacsi, N.; Ren, Q.; Dommann, A.; Beldi, G.; Maniura-Weber, K.; Rossi, R.M.; Fortunato, G. Nylon-6/chitosan core/shell antimicrobial nanofibers for the prevention of mesh-associated surgical site infection. *J. Nanobiotechnol.* **2020**, *18*, 51. [CrossRef]

122. Ghasemvand, F.; Kabiri, M.; Hassan-Zadeh, V.; Simchi, A. Chitosan, polyethylene oxide/polycaprolactone electrospun core/shell nanofibrous mat containing rosuvastatin as a novel drug delivery system for enhancing human mesenchymal stem cell osteogenesis. *Front. Mol. Biosci.* **2023**, *10*, 1220357. [CrossRef]

123. Ouerghemmi, S.; Degoutin, S.; Maton, M.; Tabary, N.; Cazaux, F.; Neut, C.; Blanchemain, N.; Martel, B. Core-Sheath Electrospun Nanofibers Based on Chitosan and Cyclodextrin Polymer for the Prolonged Release of Triclosan. *Polymers* **2022**, *14*, 1955. [CrossRef]

124. Ma, L.; Shi, X.; Zhang, X.; Dong, S.; Li, L. Electrospun Cellulose Acetate–Polycaprolactone/Chitosan Core–Shell Nanofibers for the Removal of Cr(VI). *Phys. Status Solidi (a)* **2019**, *216*, 1900379. [CrossRef]

125. Abasalta, M.; Asefnejad, A.; Khorasani, M.T.; Saadatabadi, A.R. Fabrication of carboxymethyl chitosan/poly(ε-caprolactone)/doxorubicin/nickel ferrite core-shell fibers for controlled release of doxorubicin against breast cancer. *Carbohydr. Polym.* **2021**, *257*, 117631. [CrossRef]

126. Hadjianfar, M.; Semnani, D.; Varshosaz, J.; Mohammadi, S.; Rezazadeh Tehrani, S.P. 5FU-loaded PCL/Chitosan/Fe₃O₄ Core-Shell Nanofibers Structure: An Approach to Multi-Mode Anticancer System. *Adv. Pharm. Bull.* **2022**, *12*, 568–582. [CrossRef]

127. Ghazalian, M.; Afshar, S.; Rostami, A.; Rashedi, S.; Bahrami, S.H. Fabrication and characterization of chitosan-polycaprolactone core-shell nanofibers containing tetracycline hydrochloride. *Colloids Surf. A Physicochem. Eng. Asp.* **2022**, *636*, 128163. [CrossRef]

128. Yousefi, P.; Dini, G.; Movahedi, B.; Vaezifar, S.; Mehdikhani, M. Polycaprolactone/chitosan core/shell nanofibrous mat fabricated by electrospinning process as carrier for rosuvastatin drug. *Polym. Bull.* **2022**, *79*, 1627–1645. [CrossRef]

129. Poornima, B.; Korrapati, P.S. Fabrication of chitosan-polycaprolactone composite nanofibrous scaffold for simultaneous delivery of ferulic acid and resveratrol. *Carbohydr. Polym.* **2017**, *157*, 1741–1749. [CrossRef]

130. Rastegar, A.; Mahmoodi, M.; Mirjalili, M.; Nasirizadeh, N. Platelet-rich fibrin-loaded PCL/chitosan core-shell fibers scaffold for enhanced osteogenic differentiation of mesenchymal stem cells. *Carbohydr. Polym.* **2021**, *269*, 118351. [CrossRef] [PubMed]

131. Zhu, Y.; Jiang, S.; Xu, D.; Cheng, G.; Shi, B. Resveratrol-loaded co-axial electrospun poly(ε-caprolactone)/chitosan/polyvinyl alcohol membranes for promotion of cells osteogenesis and bone regeneration. *Int. J. Biol. Macromol.* **2023**, *249*, 126085. [CrossRef] [PubMed]

132. Farboudi, A.; Nouri, A.; Shirinzad, S.; Sojoudi, P.; Davaran, S.; Akrami, M.; Irani, M. Synthesis of magnetic gold coated poly (ε-caprolactonediol) based polyurethane/poly(N-isopropylacrylamide)-grafted-chitosan core-shell nanofibers for controlled release of paclitaxel and 5-FU. *Int. J. Biol. Macromol.* **2020**, *150*, 1130–1140. [CrossRef]

133. Salsabila, D.S.; Widiyanti, P.; Hernando, E.; Hulu, I.M.; Putri Wibowo, T.D. Characterization of Coaxially Electrospun Poly (L-Lactic) Acid/Chitosan with Heparin Modification as Patch Angioplasty Candidate. *J. Membr. Sci. Res.* **2023**, *9*, 552200.

134. dos Santos, D.M.; Chagas, P.A.M.; Leite, I.S.; Inada, N.M.; de Annunzio, S.R.; Fontana, C.R.; Campana-Filho, S.P.; Correa, D.S. Core-sheath nanostructured chitosan-based nonwovens as a potential drug delivery system for periodontitis treatment. *Int. J. Biol. Macromol.* **2020**, *142*, 521–534. [CrossRef]

135. Sattari, S.; Tehrani, A.D.; Adeli, M.; Soleimani, K.; Rashidipour, M. Fabrication of new generation of co-delivery systems based on graphene-g-cyclodextrin/chitosan nanofiber. *Int. J. Biol. Macromol.* **2020**, *156*, 1126–1134. [CrossRef]

136. Kuo, T.-Y.; Jhang, C.-F.; Lin, C.-M.; Hsien, T.-Y.; Hsieh, H.-J. Fabrication and application of coaxial polyvinyl alcohol/chitosan nanofiber membranes. *Open Phys.* **2017**, *15*, 1004–1014. [CrossRef]

137. Chen, J.; Duan, H.; Pan, H.; Yang, X.; Pan, W. Two types of core/shell fibers based on carboxymethyl chitosan and Sodium carboxymethyl cellulose with self-assembled liposome for buccal delivery of carvedilol across TR146 cell culture and porcine buccal mucosa. *Int. J. Biol. Macromol.* **2019**, *128*, 700–709. [CrossRef] [PubMed]

138. Wu, S.; Shi, W.; Li, K.; Cai, J.; Xu, C.; Gao, L.; Lu, J.; Ding, F. Chitosan-based hollow nanofiber membranes with polyvinylpyrrolidone and polyvinyl alcohol for efficient removal and filtration of organic dyes and heavy metals. *Int. J. Biol. Macromol.* **2023**, *239*, 124264. [CrossRef]

139. Cai, L.; Shi, H.; Cao, A.; Jia, J. Characterization of gelatin/chitosan ploymer films integrated with docosahexaenoic acids fabricated by different methods. *Sci. Rep.* **2019**, *9*, 8375. [CrossRef] [PubMed]

140. Abasalta, M.; Zibaseresht, R.; Yousefi Zoshk, M.; Foroutan Koudehi, M.; Irani, M.; Hami, Z. Simultaneous loading of clarithromycin and zinc oxide into the chitosan/gelatin/polyurethane core–shell nanofibers for wound dressing. *J. Dispers. Sci. Technol.* **2022**, *44*, 2664–2674. [CrossRef]

141. Kaewklin, P.; Siripatrawan, U.; Suwanagul, A.; Lee, Y.S. Active packaging from chitosan-titanium dioxide nanocomposite film for prolonging storage life of tomato fruit. *Int. J. Biol. Macromol.* **2018**, *112*, 523–529. [CrossRef]

142. Râpă, M.; Gaidau, C.; Mititelu-Tartau, L.; Berechet, M.-D.; Berbecaru, A.C.; Rosca, I.; Chiriac, A.P.; Matei, E.; Predescu, A.-M.; Predescu, C. Bioactive Collagen Hydrolysate-Chitosan/Essential Oil Electrospun Nanofibers Designed for Medical Wound Dressings. *Pharmaceutics* **2021**, *13*, 1939. [CrossRef] [PubMed]

143. Avci, H.; Ghorbanpoor, H.; Nurbas, M. Preparation of origanum minutiflorum oil-loaded core–shell structured chitosan nanofibers with tunable properties. *Polym. Bull.* **2018**, *75*, 4129–4144. [CrossRef]

144. Movahedi, M.; Karbasi, S. A core-shell Electrospun Scaffold of polyhydroxybutyrate-starch/halloysite Nanotubes Containing Extracellular Matrix and Chitosan for Articular Cartilage Tissue Engineering Application. *J. Polym. Environ.* **2023**, *31*, 3052–3069. [CrossRef]

145. Abdelgawad, A.M.; Hudson, S.M.; Rojas, O.J. Antimicrobial wound dressing nanofiber mats from multicomponent (chitosan/silver-NPs/polyvinyl alcohol) systems. *Carbohydr. Polym.* **2014**, *100*, 166–178. [CrossRef]

146. Dobrovolskaya, I.P.; Yudin, V.E.; Popryadukhin, P.V.; Ivan'kova, E.M.; Shabunin, A.S.; Kasatkin, I.A.; Morgantie, P. Effect of chitin nanofibrils on electrospinning of chitosan-based composite nanofibers. *Carbohydr. Polym.* **2018**, *194*, 260–266. [CrossRef]

147. Fatullayeva, S.; Tagiyev, D.; Zeynalov, N.; Mammadova, S.; Aliyeva, E. Recent advances of chitosan-based polymers in biomedical applications and environmental protection. *J. Polym. Res.* **2022**, *29*, 259. [CrossRef]

148. Marin, L.; Andreica, B.-I.; Anisiei, A.; Cibotaru, S.; Bardosova, M.; Materon, E.M.; Oliveira, O.N. Quaternized chitosan (nano)fibers: A journey from preparation to high performance applications. *Int. J. Biol. Macromol.* **2023**, *242*, 125136. [CrossRef] [PubMed]

149. Milewska, A.; Chi, Y.; Szczepanski, A.; Barreto-Duran, E.; Dabrowska, A.; Botwina, P.; Obloza, M.; Liu, K.; Liu, D.; Guo, X.; et al. HTCC as a Polymeric Inhibitor of SARS-CoV-2 and MERS-CoV. *J. Virol.* **2021**, *95*, e01622-20. [CrossRef] [PubMed]

150. Elamri, A.; Zdiri, K.; Hamdaoui, M.; Harzallah, O. Chitosan: A biopolymer for textile processes and products. *Text. Res. J.* **2022**, *93*, 1456–1484. [CrossRef]

151. Mi, X.; Vijayaragavan, K.S.; Heldt, C.L. Virus adsorption of water-stable quaternized chitosan nanofibers. *Carbohydr. Res.* **2014**, *387*, 24–29. [CrossRef] [PubMed]

152. Yan, X.; Yao, H.; Luo, J.; Li, Z.; Wei, J. Functionalization of Electrospun Nanofiber for Bone Tissue Engineering. *Polymers* **2022**, *14*, 2940. [CrossRef] [PubMed]

153. Tamilarasi, G.P.; Sabarees, G.; Manikandan, K.; Gouthaman, S.; Alagarsamy, V.; Solomon, V.R. Advances in electrospun chitosan nanofiber biomaterials for biomedical applications. *Mater. Adv.* **2023**, *4*, 3114–3139. [CrossRef]

154. Wang, L.; Zhang, C.; Gao, F.; Pan, G. Needleless electrospinning for scaled-up production of ultrafine chitosan hybrid nanofibers used for air filtration. *RSC Adv.* **2016**, *6*, 105988–105995. [CrossRef]

155. Poshina, D.N.; Khadyko, I.A.; Sukhova, A.A.; Serov, I.V.; Zabivalova, N.M.; Skorik, Y.A. Needleless Electrospinning of a Chitosan Lactate Aqueous Solution: Influence of Solution Composition and Spinning Parameters. *Technologies* **2020**, *8*, 2. [CrossRef]

156. Bochek, A.M.; Zabivalova, N.M.; Brazhnikova, E.N.; Anferova, M.S.; Lavrent'ev, V.K. Chitosan—Polyamide Composite Nanofibers Produced by Needleless Electrospinning. *Fibre Chem.* **2019**, *50*, 391–395. [CrossRef]

157. Grimmelsmann, N.; Homburg, S.V.; Ehrmann, A. Needleless Electrospinning of Pure and Blended Chitosan. *IOP Conf. Ser. Mater. Sci. Eng.* **2017**, *225*, 012098. [CrossRef]

158. Mouro, C.; Gomes, A.P.; Gouveia, I.C. Emulsion Electrospinning of PLLA/PVA/Chitosan with Hypericum perforatum L. as an Antibacterial Nanofibrous Wound Dressing. *Gels* **2023**, *9*, 353. [CrossRef] [PubMed]

159. Lou, C.-W.; Lin, M.-C.; Huang, C.-H.; Lai, M.-F.; Shiu, B.-C.; Lin, J.-H. Preparation of Needleless Electrospinning Polyvinyl Alcohol/Water-Soluble Chitosan Nanofibrous Membranes: Antibacterial Property and Filter Efficiency. *Polymers* **2022**, *14*, 1054. [CrossRef] [PubMed]

160. Hu, J.; Prabhakaran, M.P.; Tian, L.; Ding, X.; Ramakrishna, S. Drug-loaded emulsion electrospun nanofibers: Characterization, drug release and in vitro biocompatibility. *RSC Adv.* **2015**, *5*, 100256–100267. [CrossRef]

161. Ghosh, S.; Yadav, A.; Gurave, P.M.; Srivastava, R.K. Unique Fiber Morphologies from Emulsion Electrospinning—A Case Study of Poly(ε-caprolactone) and Its Applications. *Colloids Interfaces* **2023**, *7*, 19. [CrossRef]

162. Liu, Y.; Huang, Y.; Hou, C.; Li, T.; Xin, B. The release kinetic of drug encapsulated poly(L-lactide-co-ε-caprolactone) core-shell nanofibers fabricated by emulsion electrospinning. *J. Macromol. Sci. Part A* **2022**, *59*, 489–503. [CrossRef]

163. Zhang, C.; Feng, F.; Zhang, H. Emulsion electrospinning: Fundamentals, food applications and prospects. *Trends Food Sci. Technol.* **2018**, *80*, 175–186. [CrossRef]

164. Hebishy, E.; Collette, L.; Iheozor-Ejiofor, P.; Onarinde, B.A. Stability and antimicrobial activity of lemongrass essential oil in nanoemulsions produced by high-intensity ultrasounds and stabilized by soy lecithin, hydrolyzed whey proteins, gum Arabic, or their ternary admixture. *J. Food Process. Preserv.* **2022**, *46*, e16840. [CrossRef]

165. Yoon, J.; Yang, H.-S.; Lee, B.-S.; Yu, W.-R. Recent Progress in Coaxial Electrospinning: New Parameters, Various Structures, and Wide Applications. *Adv. Mater.* **2018**, *30*, 1704765. [CrossRef]

166. Jiang, S.; Chen, Y.; Duan, G.; Mei, C.; Greiner, A.; Agarwal, S. Electrospun nanofiber reinforced composites: A review. *Polym. Chem.* **2018**, *9*, 2685–2720. [CrossRef]

167. Naeimirad, M.; Zadhoush, A.; Kotek, R.; Esmaeely Neisiany, R.; Nouri Khorasani, S.; Ramakrishna, S. Recent advances in core/shell bicomponent fibers and nanofibers: A review. *J. Appl. Polym. Sci.* **2018**, *135*, 46265. [CrossRef]

168. Ozkan, O.; Sasmazel, H.T. Antibacterial Performance of PCL-Chitosan Core-Shell Scaffolds. *J. Nanosci. Nanotechnol.* **2018**, *18*, 2415–2421. [CrossRef]

169. Morais, D.S.; Guedes, R.M.; Lopes, M.A. Antimicrobial Approaches for Textiles: From Research to Market. *Materials* **2016**, *9*, 498. [CrossRef] [PubMed]

170. Ibrahim, N.A.; El-Zairy, E.M.; Eid, B.M.; Emam, E.; Barkat, S.R. A new approach for imparting durable multifunctional properties to linen-containing fabrics. *Carbohydr. Polym.* **2017**, *157*, 1085–1093. [CrossRef]

171. Colobatiu, L.; Gavan, A.; Mocan, A.; Bogdan, C.; Mirel, S.; Tomuta, I. Development of bioactive compounds-loaded chitosan films by using a QbD approach—A novel and potential wound dressing material. *React. Funct. Polym.* **2019**, *138*, 46–54. [CrossRef]

172. Shukla, R.; Kashaw, S.K.; Jain, A.P.; Lodhi, S. Fabrication of Apigenin loaded gellan gum–chitosan hydrogels (GGCH-HGs) for effective diabetic wound healing. *Int. J. Biol. Macromol.* **2016**, *91*, 1110–1119. [CrossRef]

173. Güneş, S.; Tıhmınlıoğlu, F. Hypericum perforatum incorporated chitosan films as potential bioactive wound dressing material. *Int. J. Biol. Macromol.* **2017**, *102*, 933–943. [CrossRef] [PubMed]

174. Andreica, B.-I.; Anisiei, A.; Rosca, I.; Sandu, A.-I.; Pasca, A.S.; Tartau, L.M.; Marin, L. Quaternized chitosan/chitosan nanofibrous mats: An approach toward bioactive materials for tissue engineering and regenerative medicine. *Carbohydr. Polym.* **2023**, *302*, 120431. [CrossRef] [PubMed]

175. Xie, X.; Chen, Y.; Wang, X.; Xu, X.; Shen, Y.; Khan, A.u.R.; Aldalbahi, A.; Fetz, A.E.; Bowlin, G.L.; El-Newehy, M.; et al. Electrospinning nanofiber scaffolds for soft and hard tissue regeneration. *J. Mater. Sci. Technol.* **2020**, *59*, 243–261. [CrossRef]

176. Kazemi Asl, S.; Rahimzadegan, M.; Ostadrahimi, R. The recent advancement in the chitosan hybrid-based scaffolds for cardiac regeneration after myocardial infarction. *Carbohydr. Polym.* **2023**, *300*, 120266. [CrossRef] [PubMed]

177. Liu, Z.; Wei, W.; Tremblay, P.-L.; Zhang, T. Electrostimulation of fibroblast proliferation by an electrospun poly (lactide-co-glycolide)/polydopamine/chitosan membrane in a humid environment. *Colloids Surf. B Biointerfaces* **2022**, *220*, 112902. [CrossRef]

178. Tavakoli, M.; Labbaf, S.; Mirhaj, M.; Salehi, S.; Seifalian, A.M.; Firuzeh, M. Natural polymers in wound healing: From academic studies to commercial products. *J. Appl. Polym. Sci.* **2023**, *140*, e53910. [CrossRef]

179. Qasim, S.B.; Zafar, M.S.; Najeeb, S.; Khurshid, Z.; Shah, A.H.; Husain, S.; Rehman, I.U. Electrospinning of Chitosan-Based Solutions for Tissue Engineering and Regenerative Medicine. *Int. J. Mol. Sci.* **2018**, *19*, 407. [CrossRef]

180. Barzegar, S.; Zare, M.R.; Shojaei, F.; Zareshahrabadi, Z.; Koohi-Hosseinabadi, O.; Saharkhiz, M.J.; Iraji, A.; Zomorodian, K.; Khorram, M. Core-shell chitosan/PVA-based nanofibrous scaffolds loaded with Satureja mutica or Oliveria decumbens essential oils as enhanced antimicrobial wound dressing. *Int. J. Pharm.* **2021**, *597*, 120288. [CrossRef]

181. Jahan, I.; Zhang, L. Natural Polymer-Based Electrospun Nanofibrous Membranes for Wastewater Treatment: A Review. *J. Polym. Environ.* **2022**, *30*, 1709–1729. [CrossRef]

182. Rabiee, N.; Sharma, R.; Foorginezhad, S.; Jouyandeh, M.; Asadnia, M.; Rabiee, M.; Akhavan, O.; Lima, E.C.; Formela, K.; Ashrafizadeh, M.; et al. Green and Sustainable Membranes: A review. *Environ. Res.* **2023**, *231*, 116133. [CrossRef]

183. Phan, D.-N.; Khan, M.Q.; Nguyen, N.-T.; Phan, T.-T.; Ullah, A.; Khatri, M.; Kien, N.N.; Kim, I.-S. A review on the fabrication of several carbohydrate polymers into nanofibrous structures using electrospinning for removal of metal ions and dyes. *Carbohydr. Polym.* **2021**, *252*, 117175. [CrossRef] [PubMed]

184. Khan, M.J.; Kumari, S.; Selamat, J.; Shameli, K.; Sazili, A.Q. Reducing Meat Perishability through Pullulan Active Packaging. *J. Food Qual.* **2020**, *2020*, 8880977. [CrossRef]

185. Molognoni, L.; Daguer, H.; Motta, G.E.; Merlo, T.C.; Lindner, J.D.D. Interactions of preservatives in meat processing: Formation of carcinogenic compounds, analytical methods, and inhibitory agents. *Food Res. Int.* **2019**, *125*, 108608. [CrossRef] [PubMed]

186. Trajkovska Petkoska, A.; Daniloski, D.; D'Cunha, N.M.; Naumovski, N.; Broach, A.T. Edible packaging: Sustainable solutions and novel trends in food packaging. *Food Res. Int.* **2021**, *140*, 109981. [CrossRef] [PubMed]

187. Haghighi, H.; Licciardello, F.; Fava, P.; Siesler, H.W.; Pulvirenti, A. Recent advances on chitosan-based films for sustainable food packaging applications. *Food Packag. Shelf Life* **2020**, *26*, 100551. [CrossRef]

188. Tang, S.; Yang, J.; Lin, L.; Peng, K.; Chen, Y.; Jin, S.; Yao, W. Construction of physically crosslinked chitosan/sodium alginate/calcium ion double-network hydrogel and its application to heavy metal ions removal. *Chem. Eng. J.* **2020**, *393*, 124728. [CrossRef]

189. Yadav, N.; Monisha, M.; Niranjan, R.; Dubey, A.; Patil, S.; Priyadarshini, R.; Lochab, B. Antibacterial performance of fully biobased chitosan-grafted-polybenzoxazine films: Elaboration and properties of released material. *Carbohydr. Polym.* **2021**, *254*, 117296. [CrossRef]

190. Yu, Z.; Li, B.; Chu, J.; Zhang, P. Silica in situ enhanced PVA/chitosan biodegradable films for food packages. *Carbohydr. Polym.* **2018**, *184*, 214–220. [CrossRef]

191. Tripathi, S.; Mehrotra, G.K.; Dutta, P.K. Chitosan–silver oxide nanocomposite film: Preparation and antimicrobial activity. *Bull. Mater. Sci.* **2011**, *34*, 29–35. [CrossRef]

192. Wu, Z.; Huang, X.; Li, Y.-C.; Xiao, H.; Wang, X. Novel chitosan films with laponite immobilized Ag nanoparticles for active food packaging. *Carbohydr. Polym.* **2018**, *199*, 210–218. [CrossRef]

193. Kumar, S.; Shukla, A.; Baul, P.P.; Mitra, A.; Halder, D. Biodegradable hybrid nanocomposites of chitosan/gelatin and silver nanoparticles for active food packaging applications. *Food Packag. Shelf Life* **2018**, *16*, 178–184. [CrossRef]

194. Lou, C.; Liu, X.; Yang, C.; Ye, F.; Zhou, Q. One-step synthesis of silver nanoparticles exposed on the chitosan-covered polyamide 6 electrospinning nanofibers. *J. Appl. Polym. Sci.* **2023**, *140*, e53501. [CrossRef]

195. Sun, X.; Yin, L.; Zhu, H.; Zhu, J.; Hu, J.; Luo, X.; Huang, H.; Fu, Y. Enhanced Antimicrobial Cellulose/Chitosan/ZnO Biodegradable Composite Membrane. *Membranes* **2022**, *12*, 239. [CrossRef] [PubMed]

196. Cao, W.; Yue, L.; Wang, Z. High antibacterial activity of chitosan—Molybdenum disulfide nanocomposite. *Carbohydr. Polym.* **2019**, *215*, 226–234. [CrossRef]

197. Doğan, C.; Doğan, N.; Gungor, M.; Eticha, A.K.; Akgul, Y. Novel active food packaging based on centrifugally spun nanofibers containing lavender essential oil: Rapid fabrication, characterization, and application to preserve of minced lamb meat. *Food Packag. Shelf Life* **2022**, *34*, 100942. [CrossRef]